

**A high-resolution paleoclimate record of precipitation variability
from a stalagmite in northern Cuba spanning the late-Holocene**

by

Gregory Steltenpohl

A thesis submitted to the Graduate Faculty of
Auburn University
in partial fulfillment of the
requirements for the Degree of
Master of Science in Geology

Auburn, Alabama
May 2, 2020

Approved by

Dr. Martín Medina-Elizalde, Chair, Associate Professor of Geosciences
Dr. Ming-Kuo Lee, Robert B. Cook Professor and Department Chair of Geosciences
Dr. David T. King, Jr. , Professor of Geosciences
Dr. Sanjiv Kumar, Assistant Professor of School of Forestry and Wildlife Sciences

Abstract

I present a new stalagmite $\delta_{18}\text{O}$ record, named CL, collected from Garibaldi Cave in Matanzas, Cuba that spans between 322 and 3,747 years before present (BP). This study investigates hydroclimate drivers in Cuba and their relationship with the greater Caribbean region through correlation analyses between changes in CL stalagmite $\delta_{18}\text{O}$ to regional and global changes in surface temperatures and other climatic processes over the late Holocene. The CL $\delta_{18}\text{O}$ record is interpreted to reflect precipitation amount based on modern observations and isotopic equilibrium calculations. Analyses of the CL $\delta_{18}\text{O}$ record indicates a positive relationship between changes in Northern Hemisphere (NH) temperature and precipitation amount in Cuba over the late Holocene. A significant correlation between the CL stalagmite record and the Cariaco Basin Ti% record suggests the precipitation variability was closely linked to mean shifts in the position of the Intertropical Convergence Zone (ITCZ) during the summer and that the convective activity associated with the ITCZ was enhanced at times without a concomitant convergence center position change. In addition, we propose that precipitation changes in Cuba during the Terminal Classic Period (TCP) collapse of the Maya civilization (1200 – 950 years BP) suggest precipitation reductions in the Yucatan Peninsula lowlands and reflect Caribbean-wide precipitation reductions.

Acknowledgements

I would like to acknowledge my sincerest gratitude to the chair of my advising committee, Dr. Martín Medina-Elizalde, for his patience, enthusiasm, and encouragement throughout this project. I could not have succeeded without his invaluable mentorship and encouragement. His enthusiasm for the earth's sciences has greatly impacted me and I look forward to sharing this passion in my future.

I would also like to thank my additional committee members Dr. Ming-Kou Lee, Dr. David King, and Dr. Sanjiv Kumar who generously gave their time, advice, and criticisms. A big thank you to Dr. Matthew DeCesare for the amount of lab work you contributed to this project and for being a great travel partner to Central America. Also, thank you to Dr. Josué Polanco-Martínez who tirelessly helped me out with the numerous analyses this project required.

Thank you to the Auburn University Geology Advisory Board for granting me the GAB Research Grant, this gave me the opportunity to travel out of the country and make unforgettable memories.

Lastly, a great thank you to the Auburn University Geosciences faculty, staff, and students. Collectively, you have been a supportive and welcoming department. Thank you to all of the invaluable friendships I've made during my time at Auburn, I will always cherish the memories that we made. War Eagle!

Table of Contents

<i>Abstract</i>	2
<i>Acknowledgements</i>	3
<i>List of Tables</i>	5
<i>List of Figures</i>	6
1. Introduction	7
1.1 Relationship between precipitation amount and $\delta_{18}\text{O}$ composition	9
1.2. Background information	11
1.2.1. Cuba hydroclimate	11
1.2.2. Interannual amount effect in Cuba.....	12
1.2.3. Role of internal modes of climate variability	13
1.3. Problems and hypotheses	14
1.4. Objectives	16
2. Methods	17
2.1. Speleothem collection and location	17
2.2. Speleothem chronology	19
2.3. Stalagmite $\delta_{18}\text{O}$ composition	21
3. Results and Discussion	23
3.1. Speleothem oxygen isotope data and interpretation	23
3.2. Comparison with Temperature Records	25
3.4. Comparison with Cuban Records	33
4. Conclusion	36
5. References	37
6. Appendix	42

List of Tables

Table 1) CL Chronology	43
Table 2) Fractionation Factor Calculations	44
Table 3) Ages, $\delta^{18}\text{O}$, and $\delta^{13}\text{C}$ associated with stalagmite depth.....	45

List of Figures

Figure 1) Spatio-temporal correlation map.....	8
Figure 2) Precipitation $\delta_{18}\text{O}$ vs Precipitation Amount in Cuba	10
Figure 3) Previous Cuban Speleothem $\delta_{18}\text{O}$ records	15
Figure 4) Stalagmite CL.....	18
Figure 5) Map of Study Area	19
Figure 6) CL Age-Depth Model	20
Figure 7) Hendy Tests.....	22
Figure 8) CL stalagmite $\delta_{18}\text{O}$ and $\delta_{13}\text{C}$ records	24
Figure 9) Cross-correlation analyses	27
Figure 10) CL record vs NH Temperature Reconstructions	28
Figure 11) Wavelet Coherence Analyses.....	31
Figure 12) CL Record vs Cariaco Basin	33
Figure 13) CL Record vs Cuban Records	35

1. Introduction

This study seeks to characterize hydroclimate variability in Cuba over the last 3,747 years before present (BP). Hydroclimate variability in the Caribbean region is driven by complex atmospheric and oceanic patterns from the Atlantic and Pacific Ocean. Climatologically, the correlation between precipitation variability in Cuba and that observed in the larger Caribbean and Gulf of Mexico regions today indicates a coherent hydrological sensitivity of these regions to factors operating on large spatial scales (Fig. 1). Precipitation processes in Cuba are controlled by moisture brought into the Caribbean Sea by trade winds (easterlies) produced by the North Atlantic Subtropical High (NASH) from the Atlantic Ocean. The airflow intensifies creating the Caribbean Low-Level Jet (CLLJ) which branches during the western Caribbean summers and transports moisture northward toward the western Gulf of Mexico (Karmalkar et al., 2011; Mestas-Núñez et al., 2007; Muñoz et al., 2008; Vuille et al., 2003). The Intertropical Convergence Zone (ITCZ) oscillates in response to insolation by migrating north during the boreal summer and south during the boreal winter creating a bimodal seasonal precipitation (Philander et al., 1996; Amador, 2008). North Atlantic sea surface temperatures (SSTs) modulate the meridional temperature gradient that determines the strength of trade winds and the CLLJ, controlling the amount of moisture brought into the Caribbean basin (Oster et al., 2019). . Instrumental cyclone data indicates that the short-lived precipitation fluxes from cyclones can contribute up to 20% to western North Atlantic cumulative rainfall, including along the U.S. Gulf and Mexican coasts (Larson et al., 2005). A recent study offered paleoclimate evidence that hydroclimate variability in the Caribbean was linked to Atlantic tropical cyclone (TC) activity, whereby humid and dry intervals were associated with high and low TC frequency/intensity, respectively (Medina-Elizalde et al., 2016b). During the late Holocene, precipitation records

from the Caribbean suggest the region experienced a series of precipitation reductions that were interrupted by relatively humid conditions that may have contributed to the downfall of the Classic Maya Civilization during the Terminal Classic Period (TCP, 1250-1050 years BP) (Medina-Elizalde et al., 2010). Precipitation processes for Cuba have been characterized during the late Holocene and show that Cuba experiences a strong seasonality in precipitation which makes it an ideal location reconstruct precipitation using oxygen isotopes from speleothems (Fensterer et al., 2012a; 2012b).

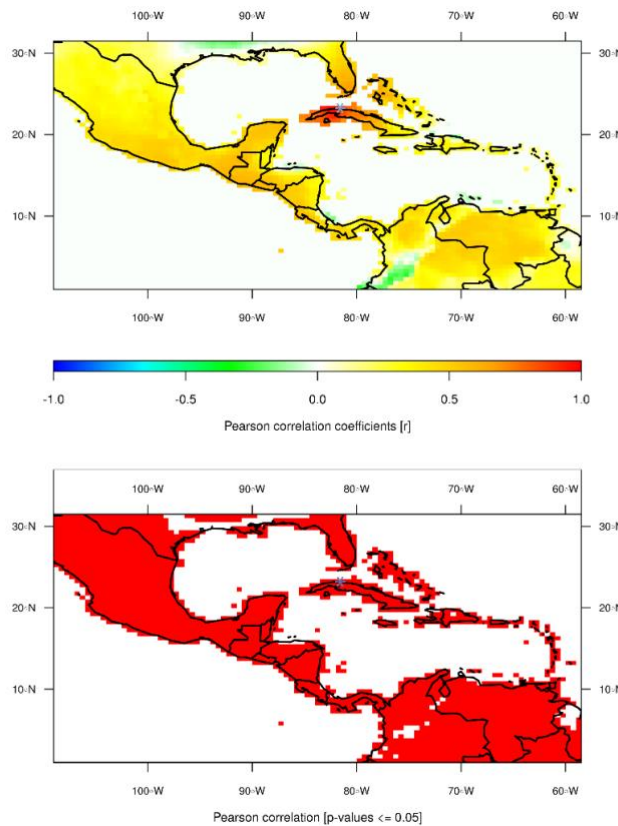


Figure 1: Spatio-temporal correlation analysis of precipitation (monthly values from 01/1901 to 12/2013 and with a spatial coverage of 0.5° latitude by 0.5° longitude) at the location (20°15'N, 87°45'W) (close to Havana, Cuba). Location of Garibaldi indicated with Green asterisk. The precipitation data set comes from the GPCC Global Precipitation Climatology Centre and is available from <https://www.esrl.noaa.gov/psd/data/gridded/data.gpcc.html>.

The Santa Calina cave system within northern Cuba is developed within a fossiliferous reef limestone platform of the Upper Pliocene–Lower Pleistocene Vedado Formation (Cabrera & Peñalver, 2001). The carbonate platform hosts biothermal limestones and clayey limestones with intercalations of calcarenites, marls and clay lenses (Pajón et al., TBA). Exposed ground above the cave system hosts Upper Pliocene and Lower Pleistocene sediments deposited in a sublittoral environment with oceanic influence and some coral growth. The carbonates that host the Santa Calina System feature a system of cracks and fissures on the preferential directions of underground caves and an epikarst zone ranging from 3 to 8 meters with variable thickness between the cave ceiling and the erosion surface. The bedrock and epikarst thicknesses and lithology in this cave system are seemingly correlated and even isochronic in origin, formation, and evolution to Río Secreto cave in the Yucatan Peninsula, whose speleothem oxygen isotopes have been analyzed as paleoclimate records of precipitation (Medina-Elizalde et al., 2017).

1.1 Relationship between precipitation amount and $\delta_{18}\text{O}$ composition

This study interprets stalagmite $\delta_{18}\text{O}$ variability by characterizing the local amount effect using available rainfall isotopic data from the International Atomic Energy Agency (IAEA), Global Network of Isotopes in Precipitation (GNIP). Available rainfall data from Cuba (2004–2015) indicates that precipitation $\delta_{18}\text{O}$ in Cuba is controlled by precipitation amount (i.e. amount effect) on seasonal and interannual time scales (Fig. 2) (Vuille et al., 2003; Lachniet, 2009).

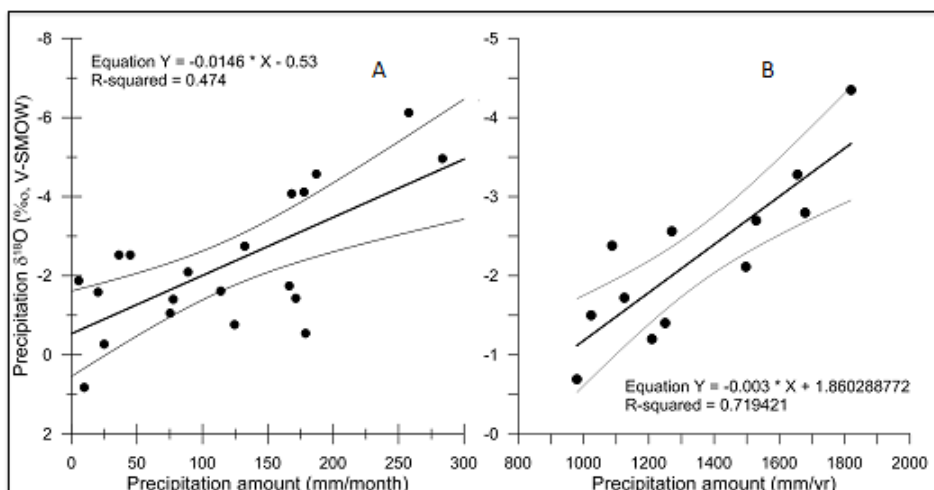


Figure 2: The IAEA GNIP instrumental database from Cuba (2004-2015) does not provide a consistently complete record of P amount and δP , but the available data suggests the existence an amount effect on seasonal time scales (Panel A) and annual time scales (Panel B). The amount effect on seasonal time scales has a similar slope observed in other locations around the Caribbean and Gulf of Mexico regions (Lachniet and Patterson, 2009; Medina-Elizalde et al., 2017; Medina-Elizalde et al., 2016a).

This implies that if it rains the same amount during five consecutive years, the precipitation $\delta_{18}\text{O}$ composition (amount weighted) is expected to remain practically unchanged. If precipitation amount changed on one given year, then precipitation $\delta_{18}\text{O}$ would change according to the amount effect relationship. Ideally, then precipitation estimates from stalagmite $\delta_{18}\text{O}$ would represent the average precipitation amount of one, two, or the number of years the calcite sample integrates. If stalagmite $\delta_{18}\text{O}$ reflects equilibrium with drip-water $\delta_{18}\text{O}$ and drip-water in turn reflects rainfall $\delta_{18}\text{O}$ on an annual or longer temporal basis, like in other Caribbean regions (Lases-Hernández et al. GCA, 2019; Lambert and Aharon, 2010; Medina-Elizalde et al., 2017), one could then estimate precipitation change from stalagmite $\delta_{18}\text{O}$ variability by shifting the annual precipitation cycle today by amounts that would yield the annual shifts in precipitation $\delta_{18}\text{O}$ that explain stalagmite $\delta_{18}\text{O}$ annual variability (Medina-Elizalde and Rohling, 2012). This requires, however, to test the assumption of isotopic equilibrium, the characterization

of the regional amount effect and an understanding of the time integration of the isotopic composition of rainfall by cave dripwater. Unfortunately, because of current travel restrictions to Cuba we are not able to monitor dripwater $\delta_{18}\text{O}$ and, therefore, this study assumes that dripwater can integrate one year of rainfall as it is observed in other studies with similar karst topography and testing isotopic equilibrium conditions using fractionation factor of $\delta_{18}\text{O}$ with the conventional Hendy Test (Hendy, 1971).

The working hypothesis underlying this study is that stalagmite $\delta_{18}\text{O}$ records from Cuba at the locale of the study area, the Santa Calina cave system, reflect hydroclimate variability of precipitation because there is a regional relationship between precipitation amount and precipitation $\delta_{18}\text{O}$ (i.e. amount effect) under equilibrium. This study reconstructs past precipitation variability from the oxygen isotopic composition of a stalagmite named CL. The CL stalagmite specimen was collected from Garibaldi cave within the Santa Calina cave system, located east of Matanzas in northern Cuba.

1.2. Background information

1.2.1. Cuba hydroclimate

Cuba has a distinctive annual cycle in precipitation characterized by the *Nortes*, *Dry* and *Rainy* seasons. The *Nortes* cold front season occurs between the months of November and February, the *Dry* season during March-April-May and the *Rainy* season between June and October. The *Rainy* season, also known as the *hurricane season*, has a bimodal distribution of precipitation with maxima during June and September and a precipitation drop by July and August, known as the midsummer drought (Magaña et al., 1999). Precipitation maxima in Cuba occur during the months of September when the Intertropical Convergence Zone reaches its northern most distribution and when the island experiences the maximum tropical cyclone

frequency. Studies with regional models and the NCEP-NCAR Global reanalysis, indicate that the dominant source of moisture for Cuba is the Caribbean Sea and is linked to the Caribbean Low Level Jet (CLLJ) (Karmalkar et al., 2011; Mestas-Nuñez et al., 2007; Muñoz et al., 2008; Vuille et al., 2003). Another source of moisture, which can dominate the seasonal and annual budget of precipitation in the northern Caribbean region, is provided by tropical waves and cyclones. Instrumental cyclone data indicates that the short-lived precipitation fluxes from cyclones can contribute up to 20% to western North Atlantic cumulative rainfall, including along the US Gulf and Mexican coasts (Larson et al., 2005). As a result, there is a statistically significant correlation ($r=0.25$, $p<0.05$) between precipitation amount and the occurrence of tropical cyclones that strike the island or pass within 60 nautical miles from its coast.

1.2.2. Interannual amount effect in Cuba

Tropical speleothem $\delta^{18}\text{O}$ measurements are used to reconstruct regional hydrological variability from seasonal to annual timescales in tropical regions (Medina-Elizalde et al., 2010; Fensterer et al., 2012a; Kennett et al., 2012; Akers et al., 2016). In particular, as mentioned previously, tropical rainfall $\delta^{18}\text{O}$ variability is inversely correlated with precipitation amount (i.e. the amount effect) in Cuba and the Caribbean region (Lachniet and Patterson, 2009; Medina-Elizalde et al., 2016a). IAEA GNIP instrumental data available in Cuba from 2004-2015 shows the existence of an amount effect slope of $\delta\text{P}/\Delta\text{P}=-0.0146\text{‰}$ on seasonal timescales and $\delta\text{P}/\Delta\text{P}=-0.003\text{‰}$ on annual timescales, whereby δP corresponds to the change in the $\delta^{18}\text{O}$ composition of rainfall associated with a change in the amount of precipitation (ΔP). The amount effect on seasonal time scales has a similar slope observed in other locations around the Caribbean and Gulf of Mexico regions (Lachniet and Patterson, 2009; Medina-Elizalde et al., 2017; Medina-Elizalde et al., 2016a).

1.2.3. Role of internal modes of climate variability

Precipitation variability in the Caribbean region has been correlated to SSTs on seasonal to multidecadal timescales in which warmer SSTs lead to increased precipitation amount due to amplified convection (Gamble et al., 2008; Lachniet, 2009). On multi-decadal timescales, one Cuban precipitation record suggests a positive relationship between precipitation amount with a North Atlantic SST multi-proxy reconstruction over the last 1,500 years (Fensterer et al., 2012a). Multi-proxy paleoclimate reconstructions accumulate regional paleoclimate data records of multiple proxies to synthesize regional and global climate trends and anomalies. Northern Hemisphere (NH) surface temperature reconstruction by Mann et al. (2008) is a multi-proxy reconstruction from over 1,200 sets of annual and decadal resolved proxy series from tree-ring, marine sediment, speleothem, lacustrine, ice core, coral, and historical records over the last 1,800 years. NH SST and Atlantic Multidecadal Variability (AMV) region SST reconstruction by Mann et al. (2009) is a multi-proxy reconstruction from over one thousand sets of proxy records in the Northern Hemisphere that cover the last 1,500. The Mann et al. (2009) reconstruction observes North Atlantic SST cooling and warming climate anomalies during the Little Ice Age (LIA; 500 – 200 years BP) and the Medieval Climate Anomaly (MCA; 1000 – 800 BP) shown in Caribbean paleoclimate records as dry and wet periods, respectively (Haug et al., 2001; Mann et al., 2009). A Caribbean wide drought during the early MCA spans from 1200 – 950 BP is suggested by a multi-proxy review from eighteen records spanning the Caribbean with an emphasis on the Yucatan Peninsula (Bhattacharya et al., 2017). This analysis also covers the time before the collapse of the Maya civilization that occurred during the Terminal Classic Period (TCP; 1250 – 1000 BP). Numerous high-resolution paleoclimate records have been produced in the Caribbean region to define late Holocene drought periods with an interest in

cultural implications during the collapse of the Maya Civilization during the Terminal Classic Period (1250 – 1000 BP)(Curtis et al., 1996; Webster et al., 2007; Akers et al., 2016; Medina-Elizalde et al., 2010; Kennett et al., 2012).

1.3. Problems and hypotheses

Hydroclimate variability in Cuba has been recorded by just two stalagmite $\delta_{18}\text{O}$ records of precipitation from sample Cuba Grande (CG)(Fensterer et al., 2012a) and Cuba Pequeño (CP)(Fensterer et al., 2012b)(Fig. 3). Both stalagmites were collected inside Dos Anas cave, west of Pinar del Rio, and should reflect similar $\delta_{18}\text{O}$ variability. However, these records show vastly different $\delta_{18}\text{O}$ values and contradicting trends. Stalagmite CG record has lower $\delta_{18}\text{O}$ values than the CP stalagmite record and the IAEA GNIP database in Cuba. Due to the lack of visible layers, a Hندی test was not performed on stalagmite CG and consequently undetermined it grew in equilibrium and may be a consequence of the remarkably low values. The CG record of precipitation shows a gradual decrease in $\delta_{18}\text{O}$ over the last 1,250 years, interpreted as an increase in precipitation over, yet an opposing increasing $\delta_{18}\text{O}$ trend is found in the CP record during this time. Similar long-term drying trends over the last 1,250 years has been recorded in the sediment titanium/iron concentration record of precipitation from the Cariaco Basin in Venezuela and is interpreted as a southward shift in the Intertropical Convergence Zone (ITCZ; Haug et al., 2001). The CG precipitation record suggests a multi-decadal relationship with changes in SSTs from the Atlantic Multidecadal Variability (AMV), a spatially dependent multidecadal variation of North Atlantic SSTs in which a positive AMV phase reflects warmer North Atlantic SSTs and therefore increased evaporation in the Caribbean, and vice versa (Knight et al., 2006; Sutton and Hodson, 2005; Lachniet, 2009; Poveda et al., 2006). Due to the large uncertainties in the later portion of CG's chronology, the record cannot be confident in

identifying relationships with the multi-proxy AMV reconstruction created by Mann et al. (2009). The CP record was unable to determine the presence of AMV variability due to its low temporal resolution. The AMV has been observed in Puerto Rico from a speleothem paleoclimate record of precipitation compared to the instrumental record of the 19th and 20th centuries (Winter et al. 2011). North Atlantic SST cooling and warming climate anomalies over the late Holocene such as the LIA and the MCA observed as cooling and warming of NH SSTs are mostly unrecognizable in the Cuban record with only the CP record recognizing the MCA as a wet event over the last 1,500 year.

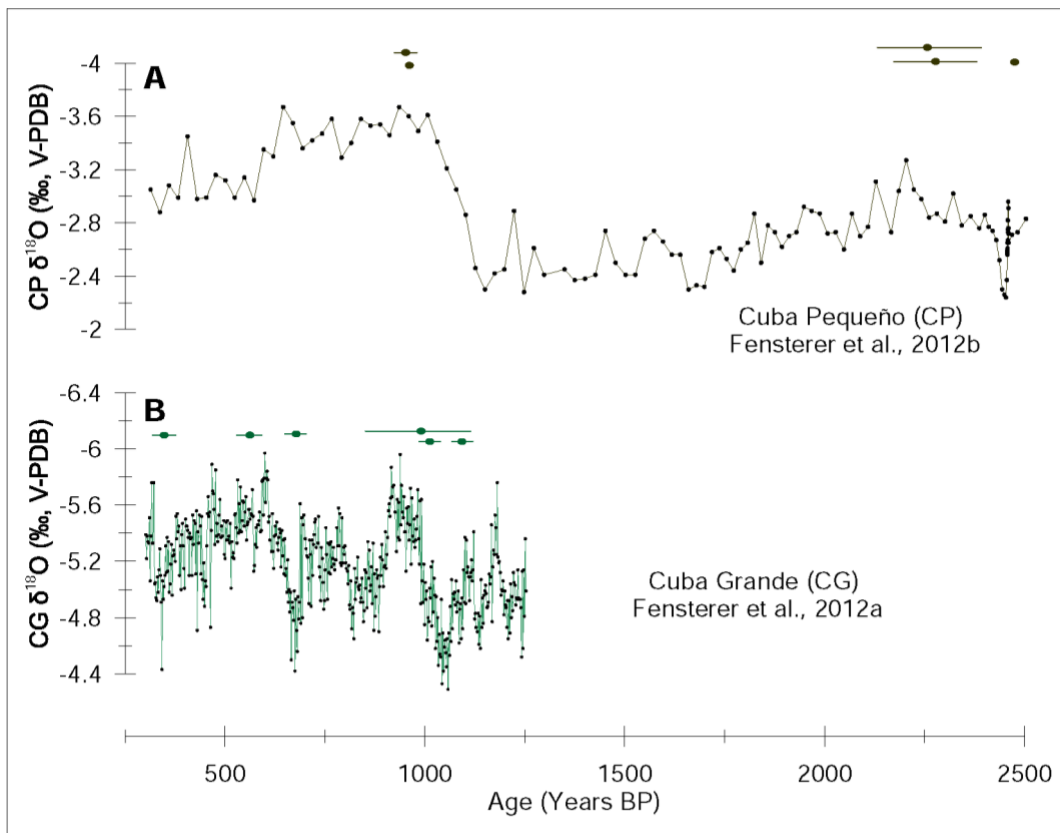


Figure 3: Previous Cuban speleothem $\delta^{18}\text{O}$ records of precipitation: stalagmite sample Cuba Pequeño (CP, Fensterer et al., 2012b) and stalagmite sample Cuba Grande (CG, Fensterer et al., 2012a).

These inconsistencies in methods and climatic interpretations of available Cuban precipitation records raises questions of legitimacy of these records. Due to the lack of any other Cuban paleoclimate records, the available records' uncertainties fail to make clear connections between Cuban precipitation variability to regional or global hydroclimate processes. Understanding hydroclimate processes of Cuba during the late Holocene can give context to studies of historic civilizations in the Caribbean region. Therefore, we need new late Holocene speleothem precipitation records from Cuba to clarify hydroclimate drivers in the Caribbean region and place Cuba in climatic context with the development and collapse of historic civilizations from the Caribbean region.

1.4. Objectives

This study exploits the unique opportunity provided by a new stalagmite $\delta_{18}\text{O}$ record to reconstruct precipitation variability spanning the late Holocene to investigate hydroclimate drivers in Cuba and their relationship with the greater Caribbean region. Particularly, this study seeks to examine correlations between changes in stalagmite $\delta_{18}\text{O}$, interpreted as changes in precipitation, to regional and global changes in surface temperatures and other climatic processes over the late Holocene to clarify what drives hydroclimate variability in Cuba.

2. Methods

2.1. Speleothem collection and location

In 2016, the 27-cm long stalagmite specimen named CL (Fig. 4), was retrieved from Garibaldi cave of the Santa Catalina cave system East of Matanzas, Cuba shown in Figure 5 (23° 4' 32.2" N; 84° 84 23' 58.4" W)(Pajón et al., TBA). The stalagmite was no longer actively growing and was harvested near its base. It was shipped to Auburn University where it was cut lengthwise and polished. The stalagmite presents visually distinctive laminations, which do not represent annual depositions as suggested by comparisons with U-Th dates.



Figure 4. The stalagmite CL used for $\delta_{18}\text{O}$ in this study. Specimen is 27-cm long. Microsamples were taken along CL's main growth axis and can be seen as a fine line running down the center.

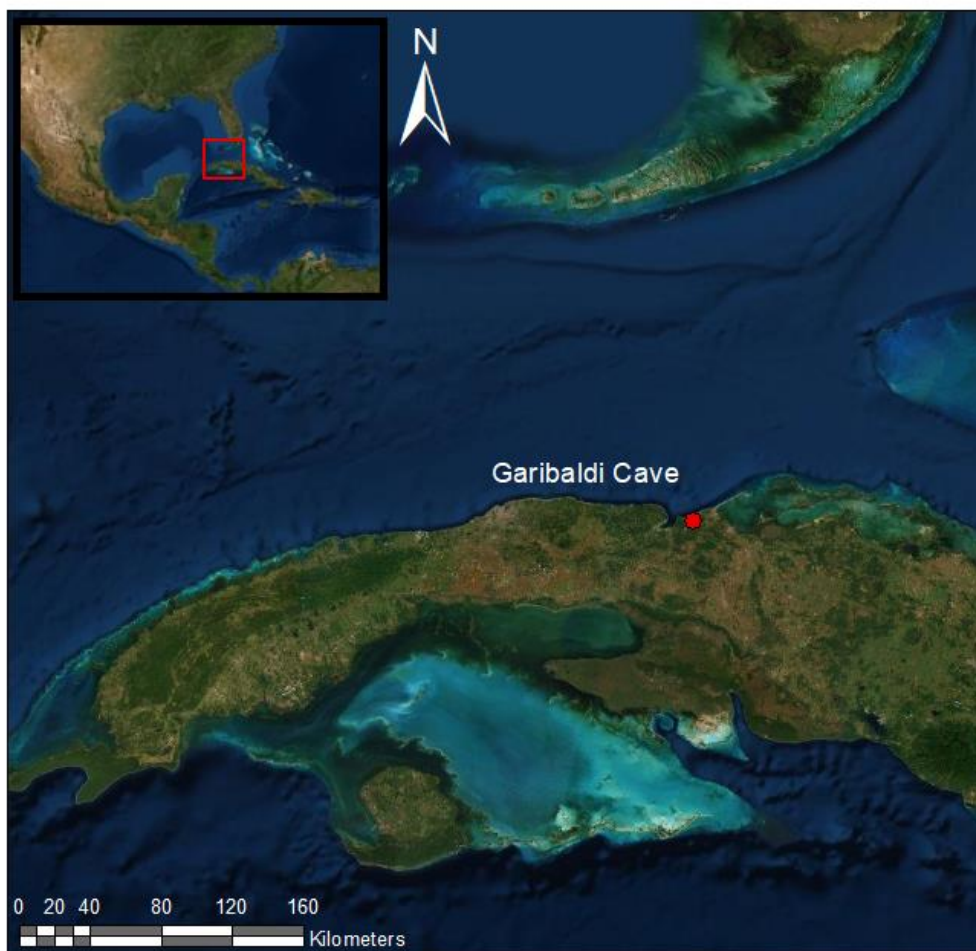


Figure 5: Map of Cuba. Red circle marks location of Garibaldi Cave located on the northern coast.

2.2. Speleothem chronology

The speleothem CL time scale was determined from 7 absolute U-Th dates (Table 1; Supplementary Material), following established methods (Cheng et al., 2013b; Shen et al., 2003, 2012). Calcite powders weighing from 60 to 150 mg were used for uranium and thorium chemistry (Shen et al., 2003). U-Th isotopic measurements were conducted on a multi-collector inductively coupled plasma mass spectrometer (MC-ICP-MS), at David McGee's Laboratory in the Massachusetts Institute of Technology (Shen et al., 2012). A triple-spike, ^{229}Th - ^{233}U - ^{236}U ,

isotope dilution method was employed to correct for mass bias and determine all uranium and thorium isotopic and concentration values in an off-line data reduction process developed by Shen et al. (2002). Dating is based on the U-Th disequilibrium technique which is based on the decay of the parent isotope ^{238}U into its daughter ^{230}Th . All errors of isotopic data and dates given are two standard deviations. Errors range from 18 to 67 years. The stalagmite CL's age model (Fig. 6) was created on 6,600,000 iterations based on Bayesian statistics using the “rbacon” package for RStudio software (Blaauw and Christen, 2011). U-Th dates suggest that CL grew continuously for 3,425 years from 322 to 3,747 years BP.

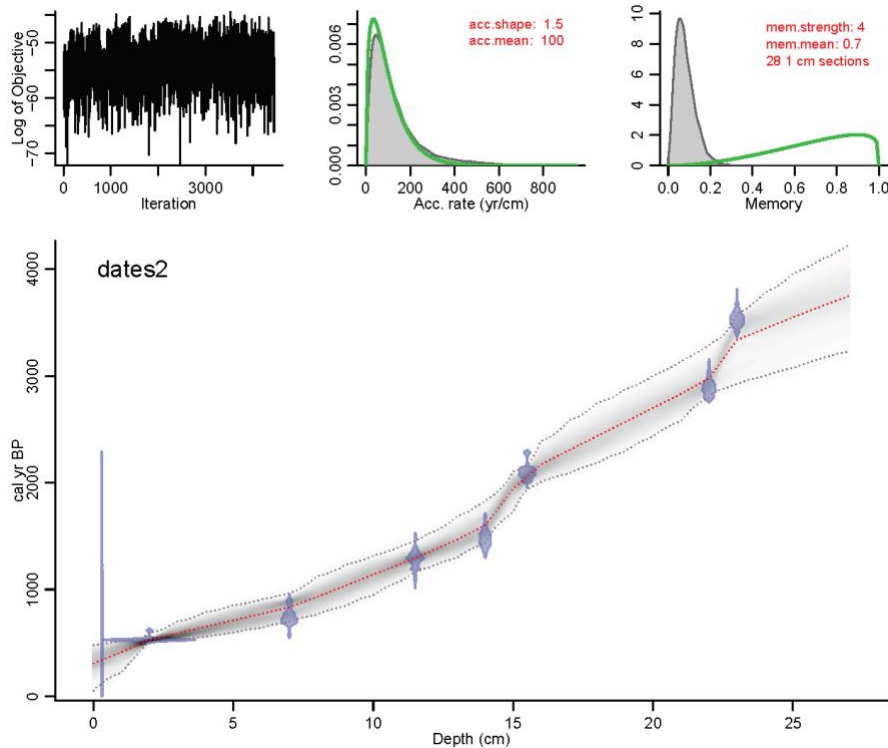


Figure 6: Stalagmite sample CL's age-depth model created by 6,600,000 iterations based on Bayesian statistics using the “rbacon” package for RStudio software giving a 95% confidence interval (Blaauw and Christen, 2011).

2.3. Stalagmite $\delta_{18}\text{O}$ composition

Stalagmite CL oxygen isotopic composition was determined from 540 calcite powder microsamples drilled along its main growth axis using a Sherline 2010 vertical mill fitted with a drill bit 0.5 and 0.8 mm in diameter. The sampling resolution was 0.5 mm, yielding an average temporal resolution of ~6 years. The oxygen isotopic composition of calcite powders was analyzed with a Thermo Scientific Delta V Plus Isotope Ratio Mass Spectrometer in Prof. Medina's laboratory in the Department of Geosciences at Auburn University. The corresponding calcite oxygen isotope ratios are recorded in delta notation per mil ($\delta_{18}\text{O}$) where $\delta_{18}\text{O}$ values are the per mil difference between the sample and the IAEA standard in delta notation where $\delta_{18}\text{O} = (R_{\text{sample}}/R_{\text{standard}} - 1) * 1000$, and R is the ratio of the minor to the major isotope. A Hendy test, used to assess whether isotopic equilibrium existed during the time of calcite deposition, was also performed along prominent laminations throughout CL where seven powder microsamples were drilled and analyzed to determine their stable isotope composition (Fig. 7).

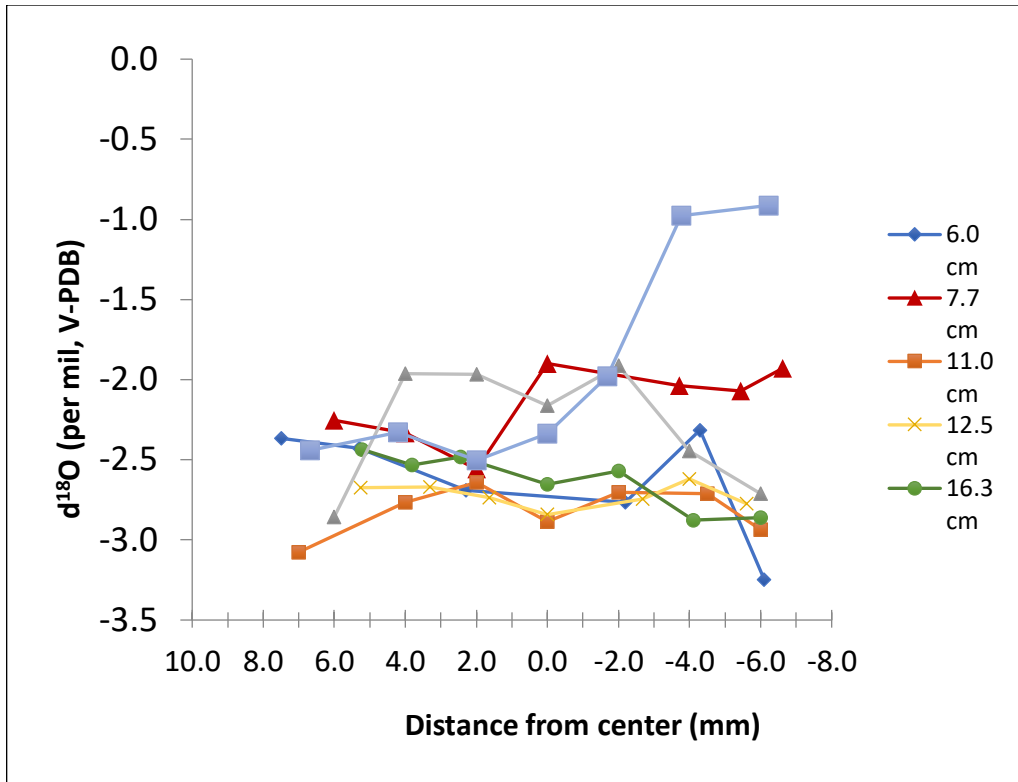


Figure 7: Hendy test on CL stalagmite. Seven laminations were sampled at the distance from the stalagmite top indicated in the legend. Lack of systematic variability in stalagmite $\delta^{18}\text{O}$ moving away from the growth axis indicates that CL grew under isotopic equilibrium values.

In addition to evidence based on the Hendy test, we find support that CL stalagmite $\delta^{18}\text{O}$ values reflect isotopic equilibrium conditions or near equilibrium, specifically by fractionation factors from Affek and Zaarur et al. (2014), Hansen et al. (2019), Tremaine et al. (2011), and Kim and O’Neil (1997). Fractionation factors can calculate speleothem $\delta^{18}\text{O}$ values in equilibrium from drip water $\delta^{18}\text{O}$ values and cave temperature. Using regional precipitation $\delta^{18}\text{O}$ values with assumed cave air temperature at 23.5° C, approximately 1° C less than the average climate of Matanzas, the expected value range for speleothem calcite falls within the values of CL calcite $\delta^{18}\text{O}$ (Table 2; Supplementary Material). Due to the fractionation factor range of drip water $\delta^{18}\text{O}$ values fall within the range of CL’s $\delta^{18}\text{O}$ values with the support of the Hendy tests,

we assume that stalagmite CL formed at or near isotopic equilibrium conditions with drip water within this cave system.

3. Results and Discussion

3.1. Speleothem oxygen isotope data and interpretation

We interpret the stalagmite $\delta_{18}\text{O}$ record to reflect variability in the local amount effect supported by instrumental observations, and therefore the amount effect previously explained. The CL stalagmite record has an average $\delta_{18}\text{O}$ of -2.42‰ , with a 2SD range from -1.55 to -3.29‰ with variability at sub-decadal and multi-decadal time scales (Fig. 8). This isotopic range is similar to that observed in the Cuba Pequeño stalagmite record from Dos Anas cave, Cuba spanning the late Holocene (Fensterer et al., 2012b). The carbon isotope response across these events could suggest hydrological shifts affecting vegetation type, density, and/or soil microbial productivity. Covariance between $\delta_{18}\text{O}$ and $\delta_{13}\text{C}$ can alternatively reflect shifts in karst hydrology whereby wetter conditions favor faster infiltration, decreased pCO_2 degassing and reduced prior calcite precipitation, ultimately producing lower $\delta_{13}\text{C}$ values (Fairchild and Treble, 2009). For this study, the CL stalagmite $\delta_{13}\text{C}$ record will be examined in support of the CL stalagmite $\delta_{18}\text{O}$ record, as we will observe $\delta_{18}\text{O}$ in context of precipitation variability in Cuba.

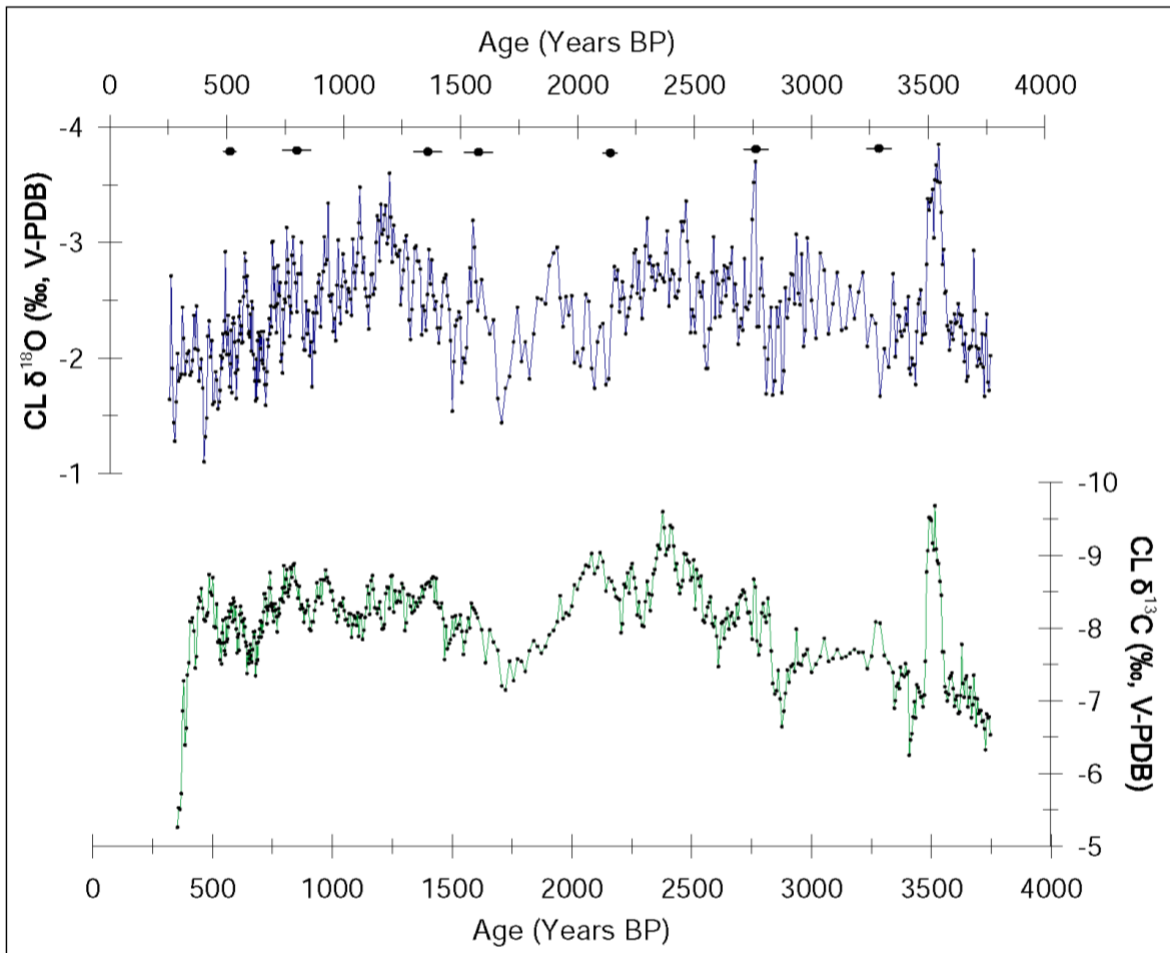


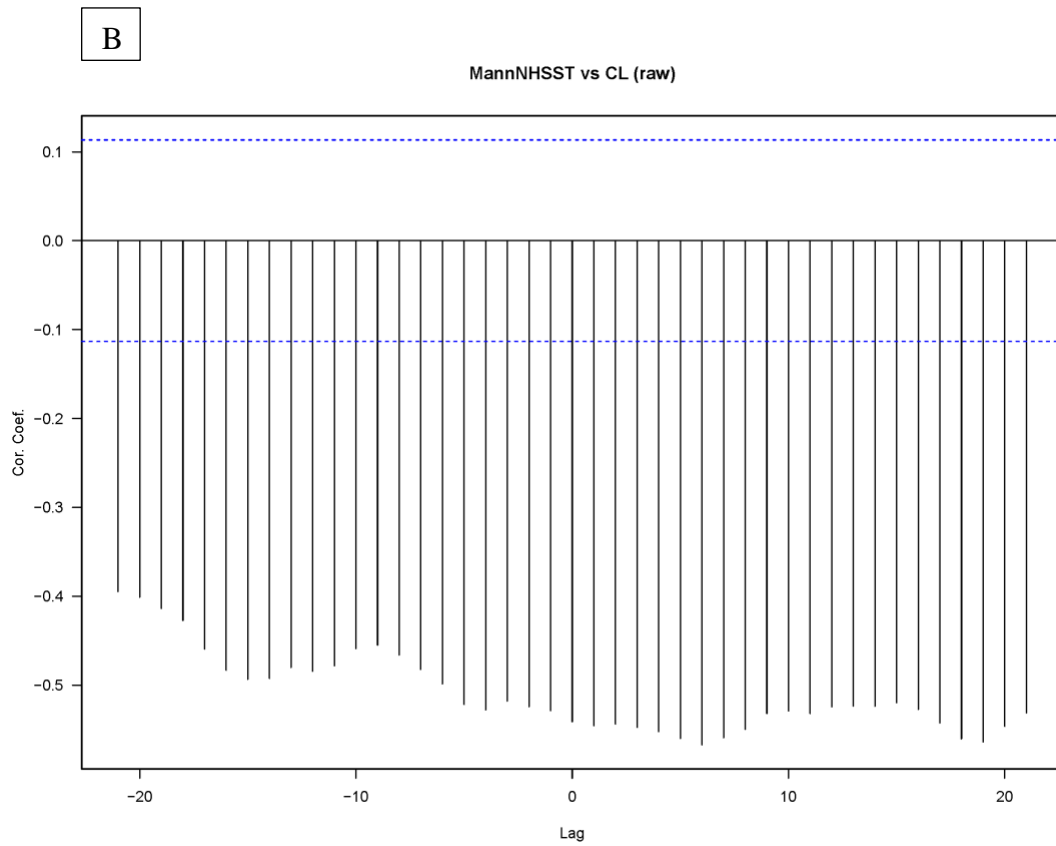
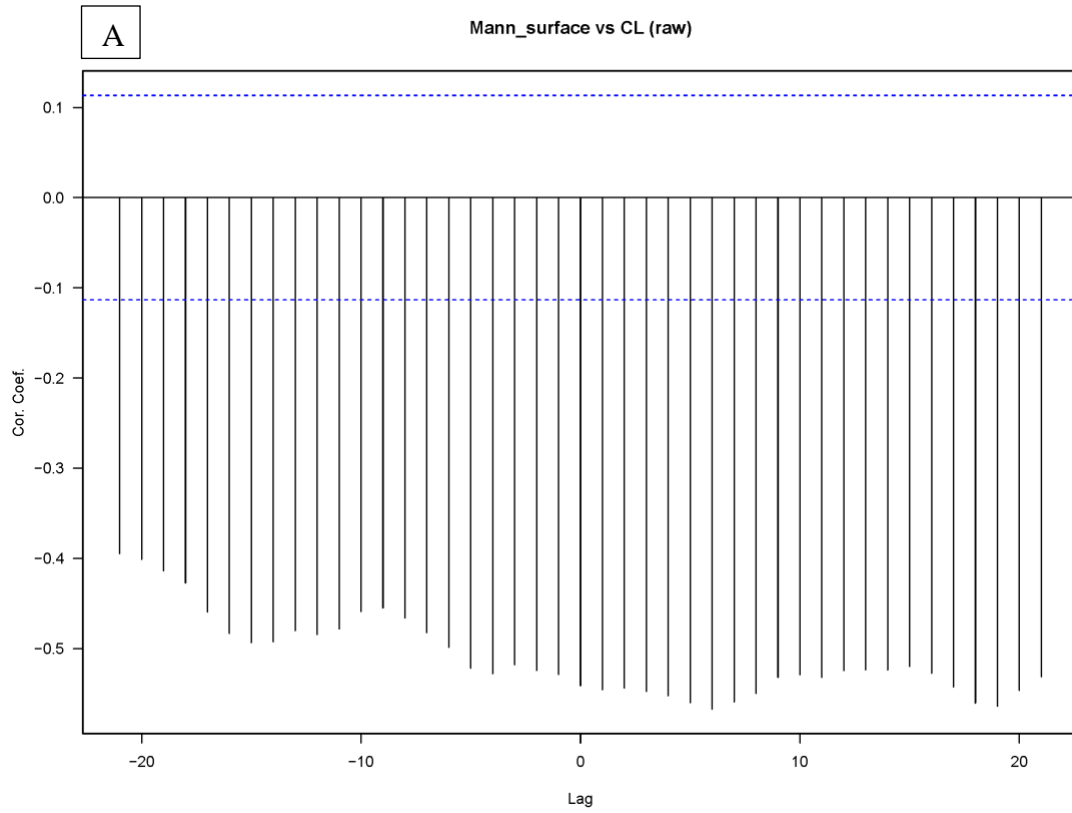
Figure 8: CL stalagmite $\delta_{18}O$ and $\delta_{13}C$ records.

The CL stalagmite record indicates anomalously low $\delta_{18}O$ intervals, interpreted as relatively wet climate conditions, from 3600 to 3490 years BP, 2770 – 2750 years BP, and 1250-1180 years BP. In contrast, the stalagmite indicates distinctive time intervals of high $\delta_{18}O$ values, which indicate dry conditions from 1800 – 1650 years BP and 500 – 322 years BP. The CL stalagmite $\delta_{18}O$ record shows a positive trend the last 1,250 years that leads to the anomalous high $\delta_{18}O$ values between and 500-322 years BP. The drying trend over the last 1,250 years BP is associated to connections of drying trends observed during the Mayan Terminal Classic Period

(TCP, 750 years BP) suggesting that the decrease in precipitation in the Maya lowlands that may have contributed to the downfall of the Mayan civilization in Central America was Caribbean wide (Curtis et al., 1996; Haug et al., 2003; Medina-Elizalde et al., 2010; Medina-Elizalde and Rohling 2012). The anomalous high $\delta_{18}\text{O}$ values, interpreted as a dry event, from 500-322 years BP in the CL stalagmite $\delta_{18}\text{O}$ record is coveval with North Atlantic atmospheric and ocean cooling during the LIA (Mann et al., 2009).

3.2. Comparison with Temperature Records

Precipitation in Cuba and the greater Caribbean has been documented to reflect changes in surface temperatures, as previously mentioned. CL stalagmite $\delta_{18}\text{O}$ record of precipitation was compared to reconstructions of NH surface temperatures (Mann et al., 2008), NH SSTs and AMV region SSTs (Mann et al., 2009). As previously explained, the NH surface temperature reconstruction by Mann et al. (2008) is a multi-proxy reconstruction from over 1,200 sets of annual and decadal resolved proxy series from tree-ring, marine sediment, speleothem, lacustrine, ice core, coral, and historical records over the last 1,800 years. The NH SST reconstruction by Mann et al. (2009) is a multi-proxy reconstruction from over one thousand sets of proxy records in the Northern Hemisphere over the last 1,500 years to observe LIA and MCA anomalies. Mann et al. (2009) also created reconstruction of changes in SSTs in the AMV region of the North Atlantic. Cross correlation results suggest that the CL stalagmite $\delta_{18}\text{O}$ record are synchronous with a significant negative correlation (CI 95%) at lag zero equaling (Fig. 9A) $r=-0.56$ for NH Surface temperature, (Fig. 9B) $r=-0.40$ for NH SST, and (Fig. 9C) $r=-0.39\%$ for AMV region SSTs.



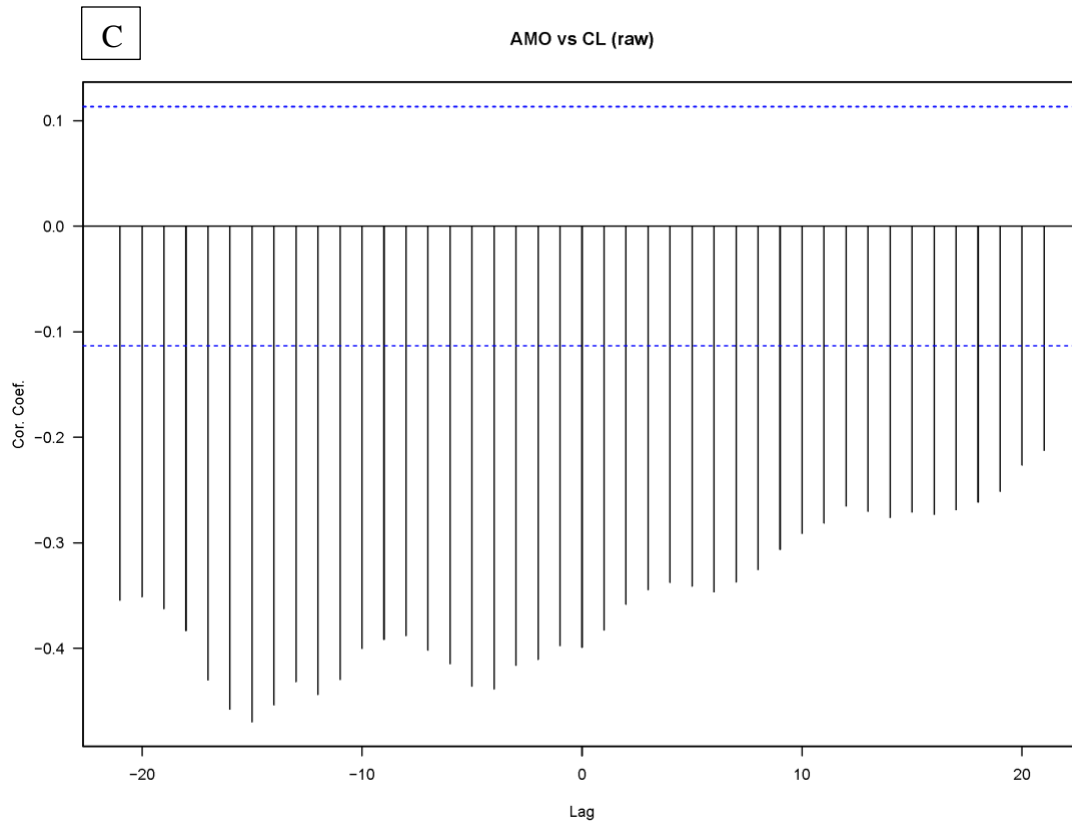


Figure 9: Cross-correlation analyses between sample CL stalagmite $\delta_{18}\text{O}$ record to: 9A) NH surface temperature reconstruction (Mann et al., 2008); 9B) NH SST reconstruction (Mann et al., 2009); and 9C) Atlantic Multidecadal Variability (AMV) region SST reconstruction (Mann et al., 2009).

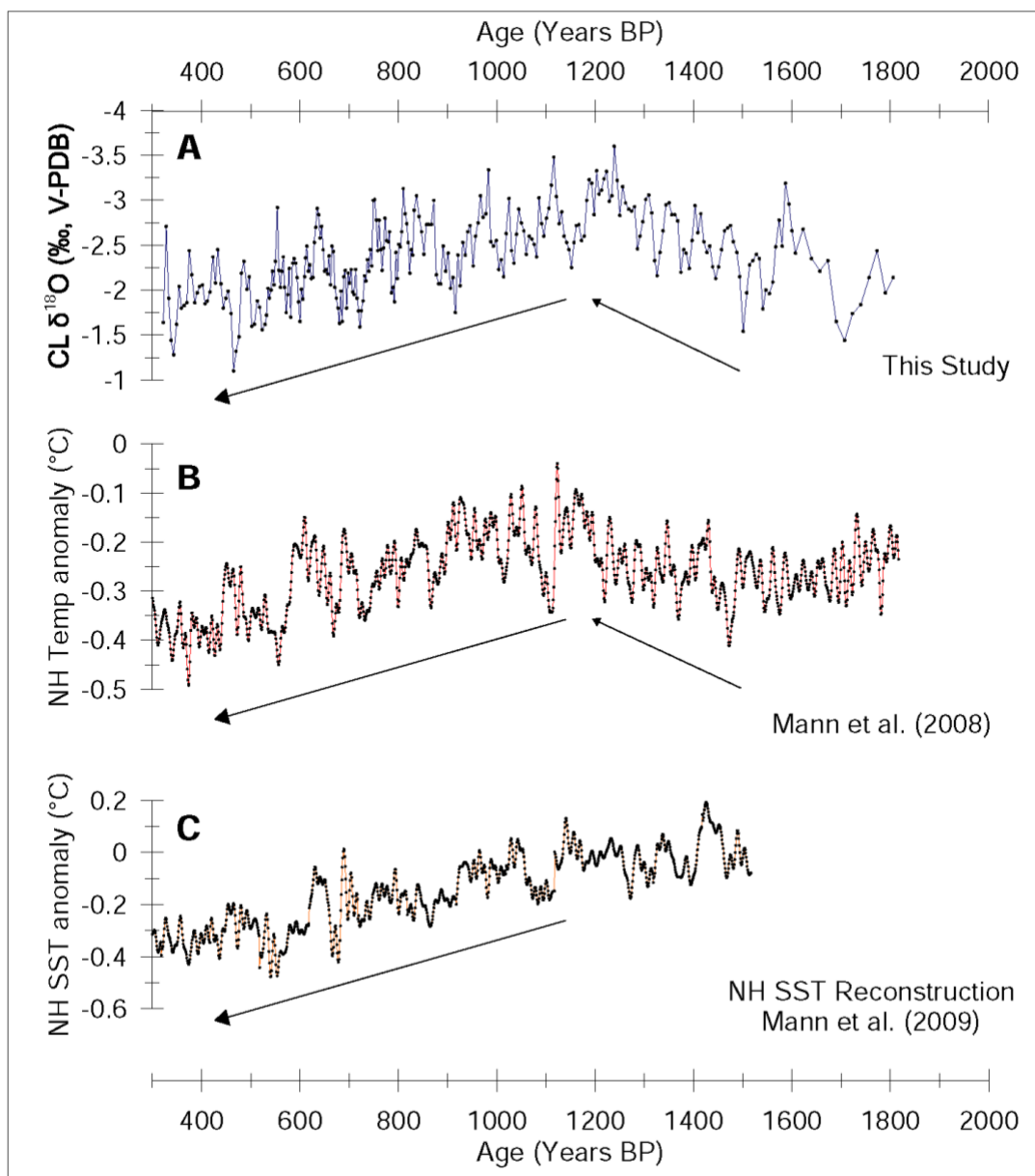
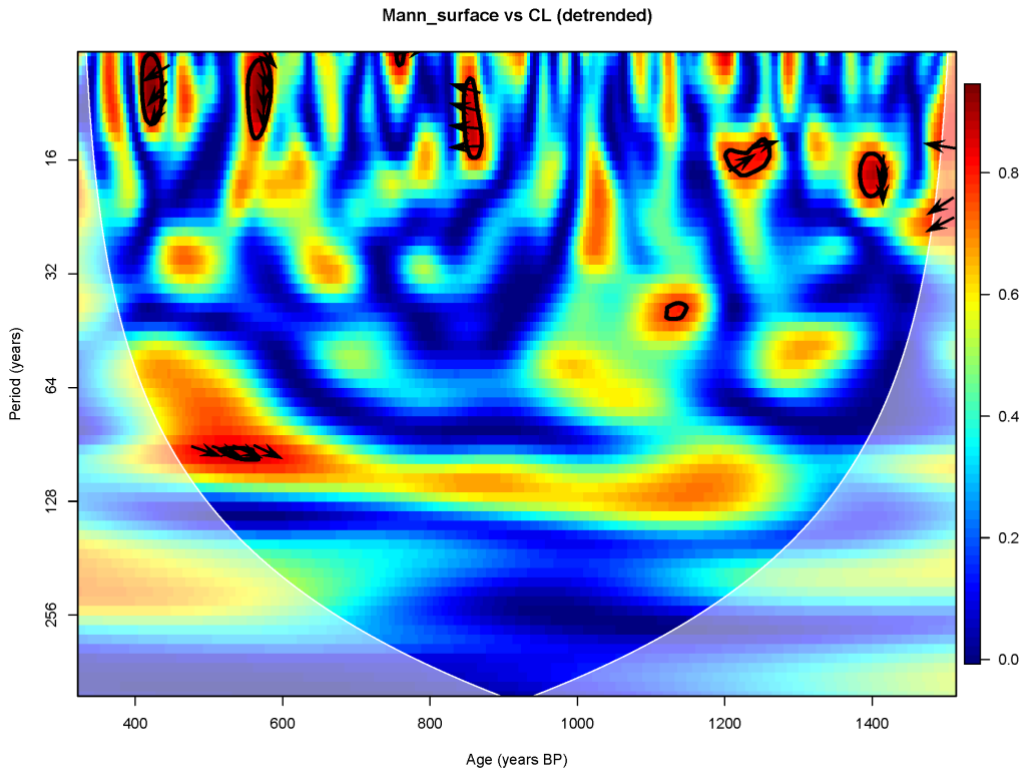


Figure 10: CL stalagmite $\delta^{18}\text{O}$ record of precipitation compared to NH Surface Temperature reconstruction by Mann et al. (2008) and NH SST reconstruction by Mann et al. (2009).

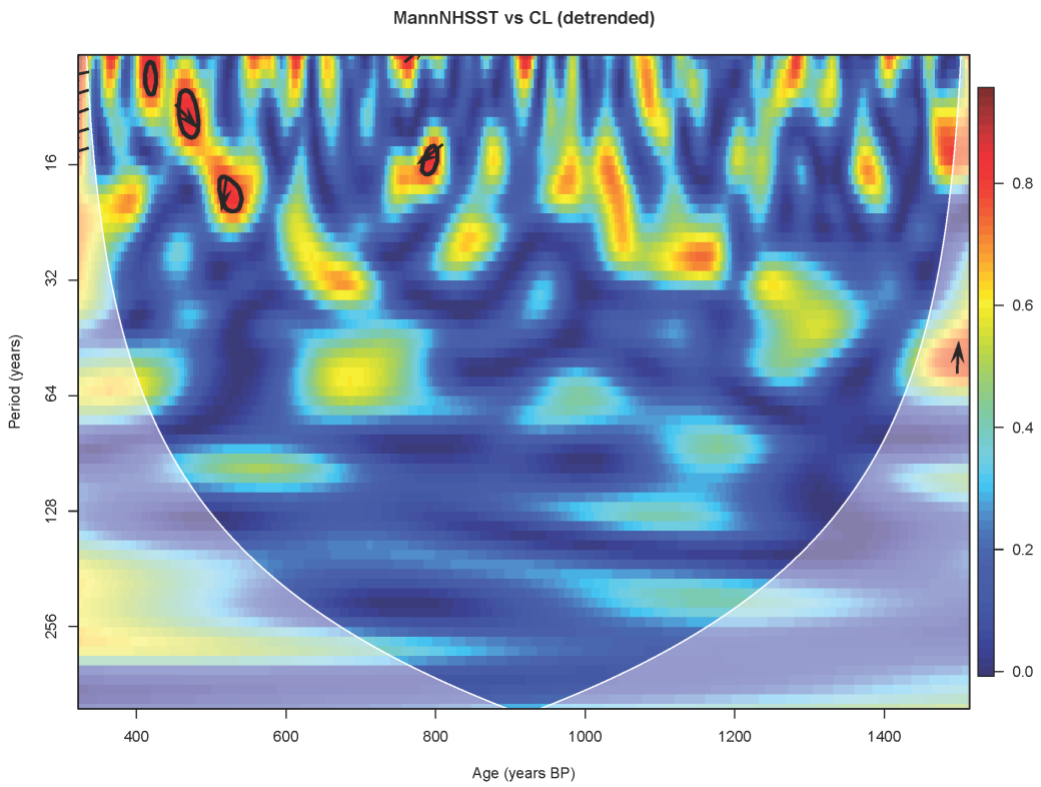
Upon visual observation between CL stalagmite $\delta^{18}\text{O}$ record of precipitation and NH surface and NH SST reconstructions, surface temperature-cooling is associated with a CL

stalagmite $\delta_{18}\text{O}$ record increasing trend over the last 1,200 years (Fig. 10). This trend is in agreement with the sediment titanium/iron concentration record of the Cariaco Basin interpreted to reflect a southward shift of the ITCZ, particularly during its summer position (Peterson and Haug, 2006). The CL stalagmite $\delta_{18}\text{O}$ record and Mann et al. (2008) NH surface records show a coeval pattern whereby a multicentennial temperature rise is associated with a CL $\delta_{18}\text{O}$ decreasing trend from 1500 to 1200 years BP. This warming trend is not observed either in the Cariaco Basin Ti and Fe percent records and the NH SST reconstructions. Wavelet Coherence (WCO) analyses (Fig. 11) show strong (>0.8 power) sub-decadal and multidecadal variability and a considerable centennial variability from 300 to 1,500 years BP between CL stalagmite $\delta_{18}\text{O}$ record and Mann et al. (2008) NH surface temperature reconstruction (Fig. 11A). The WCO analysis between CL and NH SST record (Mann et al. 2009), sub-decadal to 32-year periodicities occur later in the analyses between the CL record and the SST, yet not as significant as the relationship with NH surface temperature reconstruction (Fig. 11B). The CL record does not show strong multi-decadal variability with AMV region SSTs before 600 years BP, but coherent 128-256-year periods are seen over the duration of the AMV region reconstruction (Fig. 11C). This suggests that a climate phenomenon contributing to NH surface temperatures is driving hydroclimate variability in Cuba that is not reflected in changes in SSTs. Observed different trends early in the NH temperature and SST records can reflect the lack of sufficient spatial representation of the few available SST records within the NH (Mann et al., 2008; Mann et al., 2009). The close agreement between a terrestrial hydroclimate record from Cuba (CL stalagmite $\delta_{18}\text{O}$ record) and NH surface temperatures throughout the 2 thousand year length of these records, however, suggest a strong connection that likely stems from shifts in tropical North Atlantic SSTs.

A



B



C

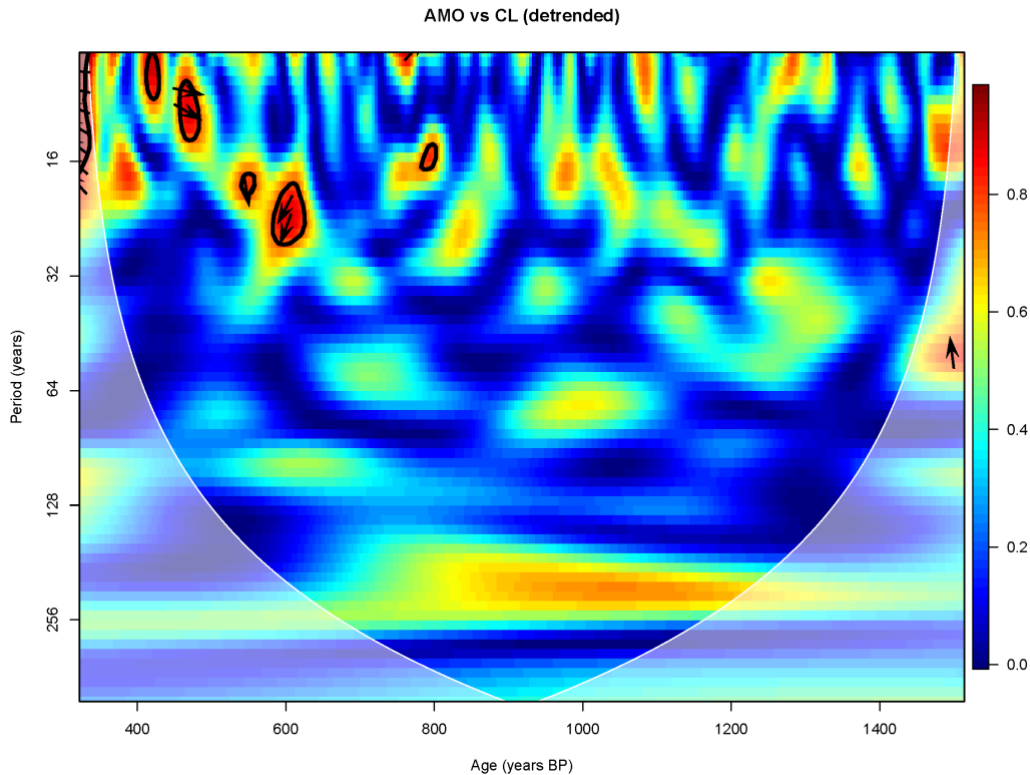


Figure 11: Wavelet Coherence (WCO) analyses between sample CL stalagmite $\delta_{18}\text{O}$ record relative to: (A) NH surface temperature reconstruction (Mann et al., 2008); (B) NH SST reconstruction (Mann et al., 2009); and (C) Atlantic Multidecadal Variability (AMV) region SST reconstruction (Mann et al., 2009). The scale on the right gives the strength (power) at different periods over a given time.

3.3. Comparison with the ITCZ

We find that distinctive long-term hydroclimate trends and events in the CL stalagmite $\delta_{18}\text{O}$ record align with the titanium/iron percent records from the Cariaco Basin, Venezuela, which is interpreted to reflect summer precipitation changes in response to persistent shifts in the position of the Intertropical Convergence Zone (ITCZ) and its belt of convective activity (Haug et al., 2001; Fig. 12). Early in the record, low CL stalagmite $\delta_{18}\text{O}$ values and high Ti% from 3700 – 3500 years BP and 2750 – 2900 years BP suggest periods of high precipitation in Cuba resulting from a more northward position of the ITCZ during the summer, Rainy season in Cuba.

High coherent precipitation variability on multi-decadal timescales between 3300 – 3100 years BP are shown between these records. Increase in CL stalagmite $\delta_{18}\text{O}$ values align with decrease in Ti% in the Cariaco Basin sediment record over the last 1,250 years. Between 2500 – 1500 years BP, the CL stalagmite $\delta_{18}\text{O}$ record shows a period of low temporal resolution and increasing $\delta_{18}\text{O}$ yet the Cariaco Basin Ti% record remains relatively stable. Visual correlation between these records suggest shifts in the ITCZ have affected precipitation in Cuba for most of the late Holocene. The absence of correlation between the Cariaco Basin Ti% record and the CL stalagmite isotopic record between 2500 – 1500 years BP, suggests an increase in the convective activity associated with the ITCZ without a concomitant displacement of its mean position. Warmer Caribbean SSTs per se, particularly in the subtropical regions, would increase moisture availability and precipitation without shifting the ITCZ.

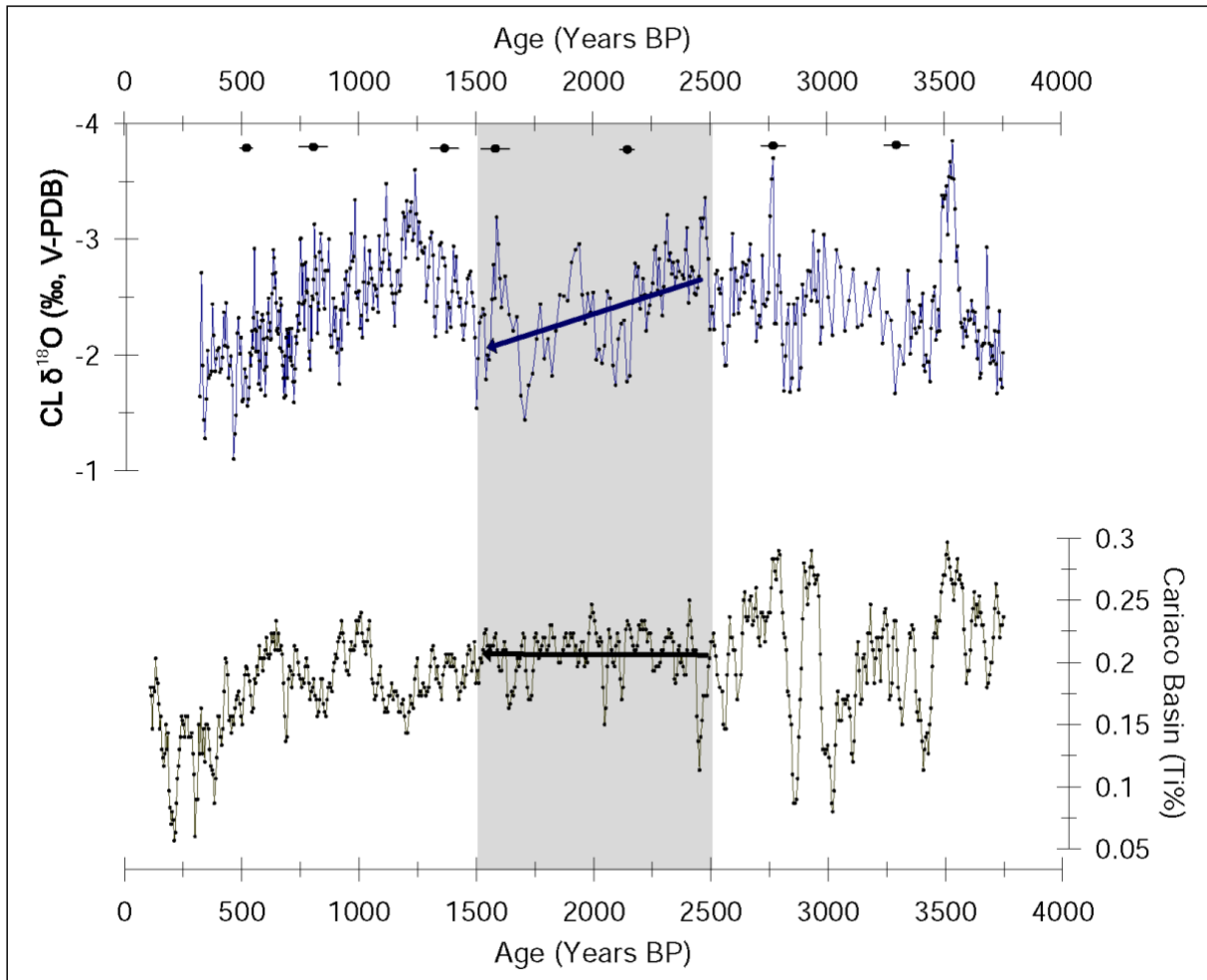


Figure 12: Speleothem sample CL $\delta^{18}\text{O}$ record compared to Cariaco Basin sediment titanium percent record over the last 3,747 years.

3.4. Comparison with Cuban Records

Previous paleoclimate records of precipitation from Cuba suggest contradicting trends that do not clarify what drives hydroclimate variability in the region on long-time scales (Fig. 13). The CL stalagmite $\delta^{18}\text{O}$ record shows higher mean $\delta^{18}\text{O}$ values (-2.4‰) than stalagmite CG $\delta^{18}\text{O}$ (-5.2‰) record but similar values mean and amplitude variability regarding the CP stalagmite $\delta^{18}\text{O}$ record (-2.8‰). The CL and CP stalagmite $\delta^{18}\text{O}$ records share similar positive isotopic trends suggesting a long-term precipitation reduction over the last 1,250 years.

Contrasting, the Cuba Grande (CG) $\delta_{18}\text{O}$ record of precipitation shows a gradual long-term decrease of $\delta_{18}\text{O}$ values suggesting that Cuba was gaining average precipitation amount during the growth of the record. All stalagmite isotope records, however, suggest a positive trend punctuated by more rapid positive isotope excursions during between 600 years BP and 300 years BP. This interval of reduced precipitation in Cuba is coveval the LIA time interval, and probably reflects North Atlantic cooling in combination with a southward displacement of the ITCZ, particularly during the summer (Paterson and Haug, 2006; Mann et al., 2009). The ~200 year variability of recognizable (0.6-0.8) power is observed between the CG and CL records. This bicentennial variability has been observed in the CG stalagmite $\delta_{18}\text{O}$ record (Fensterer et al., 2012a) interpreted to reflect the influence of solar variability.

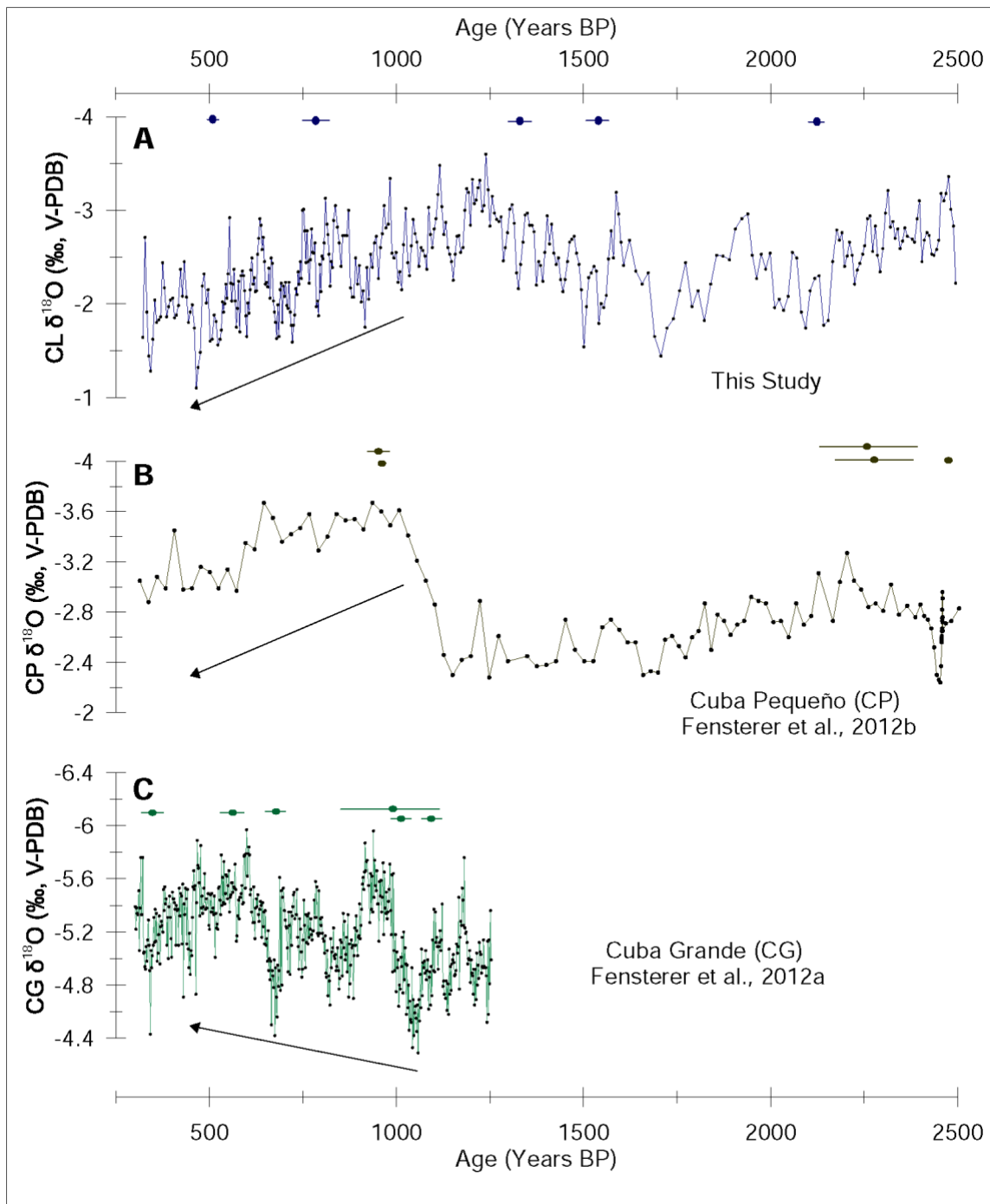


Figure 13: Speleothem sample CL $\delta^{18}\text{O}$ record compared to previous existing Cuban stalagmite $\delta^{18}\text{O}$ records: Cuba Pequeño (CP, Fensterer et al., 2012b) and Cuba Grande (CG, Fensterer et al., 2012a).

4. Conclusion

This study presents new high-resolution stalagmite $\delta_{18}\text{O}$ and $\delta_{13}\text{C}$ records from the province of Matanzas in Cuba, spanning the time interval between 322 and 3,747 years BP. Analyses of the CL $\delta_{18}\text{O}$ record and NH field-climate reconstructions indicate a positive relationship between changes in NH temperature and precipitation amount in Cuba over the late Holocene. The CL stalagmite $\delta_{18}\text{O}$ record shows better correlation between the NH surface temperature reconstruction than the SST reconstructions, suggesting that the NH SST record fails to fully capture ocean temperature variability in Caribbean region, particularly between 1400 and 1200 years BP. A significant correlation between the CL stalagmite isotopic records and the Cariaco Basin Ti% record suggests the precipitation variability was closely linked to mean shifts in the position of the ITCZ during the summer, and that the convective activity associated with the ITCZ was enhanced at times without a concomitant convergence center position change. The CL and CP stalagmite precipitation records support a drying trend over the last 1,250 years in Cuba also suggested by the Cariaco Basin Ti% record. All three available stalagmite $\delta_{18}\text{O}$ records from Cuba suggest dry conditions during the LIA time interval, reflecting North Atlantic cooling and a southward displacement of the ITCZ during the summer. The CL stalagmite $\delta_{18}\text{O}$ record suggest that Cuba became progressively drier during the Terminal Classic Period collapse of the Maya civilization (1200 – 950 years BP) suggesting precipitation reductions in the Yucatan Peninsula lowlands reflect Caribbean-wide precipitation reductions.

5. References

- Affek, H.P. and Zaarur, S., 2014, Kinetic isotope effect in CO₂ degassing: Insight from clumped and oxygen isotopes in laboratory precipitation experiments. *Geochimica et Cosmochimica Acta*, 143, pp.319-330.
- Akers, P.D., Brook, G.A., Railsback, L.B., Liang, F., Iannone, G., Webster, J.W., Reeder, P.P., Cheng, H. and Edwards, R.L., 2016, An extended and higher-resolution record of climate and land use from stalagmite MC01 from Macal Chasm, Belize, revealing connections between major dry events, overall climate variability, and Maya sociopolitical changes. *Palaeogeography, palaeoclimatology, palaeoecology*, 459, pp.268-288.
- Amador, J. A., 2008, The Intra-Americas Sea Low-level Jet Overview and Future Research. *Annals of the New York Academy of Sciences*, 1146(1), 153-188.
- Bhattacharya, T., Chiang, J.C. and Cheng, W., 2017, Ocean-atmosphere dynamics linked to 800–1050 CE drying in mesoamerica. *Quaternary Science Reviews*, 169, pp.263-277.
- Blaauw, M. and Christen, J.A., 2013, Bacon Manual v2. 2. Blaauw, M., Wohlfarth, B., Christen, J.A., Ampel, L., Veres, D., Hughen, K.A., Preusser, F., et al.(2010),—Were Last Glacial Climate Events Simultaneous between Greenland and France, pp.387-394.
- Cabrera, M. and Peñalver, L., 2001, Contribución a la estratigrafía de los depósitos cuaternarios de Cuba. *Revista Cuaternario y Geomorfología*, 15(3-4), pp.37-49.
- Cheng, H., Edwards, R.L., Shen, C.-C., Polyak, V.J., Asmerom, Y., Woodhead, J., Hellstrom, J., Wang J., Y., Kong, X.G., Spötl, C., Wang, X.F., and Alexander, E.C., 2013, Improvements in ²³⁰Th dating, ²³⁰Th and ²³⁴U half-life values, and U-Th isotopic measurements by multi-collector inductively coupled plasma mass spectrometry.: *Earth and Planetary Science Letters*, v. 372, p. 82–91.
- Curtis, J. H., Hodell, D.A., Brenner, M., 1996, Climate variability on the Yucatan peninsula (Mexico) during the past 3500 years, and implications for Maya cultural evolution. *Quaternary Research* 46: 37–47.
- Fairchild, I., and Treble, P., 2009, Trace elements in speleothems as recorders of environmental change: *Quaternary Science Reviews*, v. 28, p. 449-468.
- Fensterer, C., Scholz, D., Hoffmann, D., Spötl, C., Pajon, J., Mangini, A., 2012, Cuban stalagmite suggests relationship between Caribbean precipitation and the Atlantic Multidecadal Oscillation during the past 1.3 ka. *The Holocene* 22, 1403–1410.
- Fensterer, C., Scholz, D., Hoffmann, D.L., Spötl, C., Schröder-Ritzrau, A., Horn, C., Pajón, J.M., Mangini, A., 2012b, Millennial-scale climate variability during the last 12.5 ka recorded in a Caribbean speleothem. *Earth and Planetary Science Letters* 361, 143-151.

- Gamble, D.W., Parnell, D.B., and Curtis, S., 2008, Spatial variability of the Caribbean mid-summer drought and relation to north Atlantic high circulation. *International Journal of Climatology* 28: 343–350.
- Hansen, A., Barnett, K., Jantz, P., 2019, Global humid tropics forest structural condition and forest structural integrity maps. *Sci Data* 6, 232 <https://doi.org/10.1038/s41597-019-0214-3>
- Hodell, D.A., Anselmetti, F.S., Ariztegui, D., Brenner, M., Curtis, J.H., Gilli, A., Grzesik, D.A., Guilderson, T.J., Müller, A.D., Bush, M.B., Correa-Metrio, A., Escobar, J., and Kutterolf, S., 2008, An 85-ka record of climate change in lowland Central America: Quaternary Science Reviews, v. 27, p. 1152–1165, doi: 10.1016/j.quascirev.2008.02.008.
- Karmalkar, A. V., Bradley, R. S., and Diaz, H. F., 2011, Climate change in Central America and México: regional climate model validation and climate change projections: *Climate Dynamics*, v. 37, p. 605-629.
- Kim, S.T. and O'Neil, J.R., 1997, Equilibrium and nonequilibrium oxygen isotope effects in synthetic carbonates. *Geochimica et cosmochimica acta*, 61(16), pp.3461-3475.
- Knight, J.R., Folland, C.K., and Scaife, A.A., 2006, Climate impacts of the Atlantic Multidecadal Oscillation. *Geophysical Research Letters* 33: L17706, doi: 10.1029/2006GL026242.
- Lachniet, M.S., and Patterson, W.P., 2009, Oxygen isotope values of precipitation and surface waters in northern Central America (Belize and Guatemala) are dominated by temperature and amount effects: *Earth and Planetary Science Letters*, v. 284, p. 435–446, doi: 10.1016/j.epsl.2009.05.010.
- Lachniet, M.S., 2009, Climatic and environmental controls on speleothem oxygen-isotope values: *Quaternary Science Reviews*, v. 28, p. 412–432, doi: 10.1016/j.quascirev.2008.10.021.
- Lambert, J.W., and Aharon, P., 2010, Oxygen and hydrogen isotopes of rainfall and dripwater at DeSoto Caverns (Alabama, USA); Key to understanding past variability of moisture transport from the Gulf of Mexico: *Geochimica et Cosmochimica Acta*, v. 74, p. 846–861.
- Larson, J., Zhou, Y., and Higgins, W. R., 2005, Characteristics of Landfalling Tropical Cyclones in the United States and Mexico: *Climatology and Interannual Variability: Journal of Climate*, v. 18, no. 1247-1262.
- Lases-Hernández, F., Medina-Elizalde, M., Burns, S., Bernal-Uruchurtu, J.P., and Beddows, P., TBD, Monitoring Rio Secreto Cave System in the Yucatan Peninsula to Calibrate Paleoclimatic Proxies: *Geochimica et Cosmochimica Acta*.
- Magaña, V., Amador, A. J., and Medina, S., 1999, The Midsummer Drought over Mexico and

- Central America: *Journal of Climate*, v. 12, p. 1577-1588.
- Mann, M.E., Zhang, Z., Hughes, M.K., Bradley, R.S., Miller, S.K., Rutherford, S. and Ni, F., 2008, Proxy-based reconstructions of hemispheric and global surface temperature variations over the past two millennia. *Proceedings of the National Academy of Sciences*, 105(36), pp.13252-13257.
- Mann, M.E., Zhang, Z., Rutherford, S., Bradley, R.S., Hughes, M.K., Shindell, D., Ammann, C., Faluvegi, G. and Ni, F., 2009, Global signatures and dynamical origins of the Little Ice Age and Medieval Climate Anomaly. *Science*, 326(5957), pp.1256-1260.
- Medina-Elizalde, M., Burns, S.J., Lea, D.W., Asmerom, Y., von Gunten, L., Polyak, V., Vuille, M., Karmalkar, A., 2010, High resolution stalagmite climate record from the Yucatan Peninsula spanning the Maya terminal classic period. *Earth Planet. Sci. Lett.* 298, 255–262.
- Medina-Elizalde, M., and Rohling, E.J., 2012, Collapse of Classic Maya Civilization Related to Modest Reduction in Precipitation: *Science*, doi: 10.1126/science.1216629.
- Medina-Elizalde, M., Burns, S. J., Polanco-Martínez, J. M., Beach, T., Lases-Hernández, F., Shen, C.-C., and Wang, H.-C., 2016a, High-resolution speleothem record of precipitation from the Yucatan Peninsula spanning the Maya Preclassic Period: *Global and Planetary Change*, v. 138, p. 93-102.
- Medina-Elizalde, M., Polanco-Martinez, J. M., Lases-Hernandez, F., Bradley, R., and Burns, S., 2016b, Testing the "tropical storm" hypothesis of Yucatan Peninsula climate variability during the Maya Terminal Classic Period: *Quaternary Research*, v. 86, no. 2, p. 111-119.
- Medina-Elizalde, M., Burns, S.J., Polanco-Martinez, J., Lases-Hernandez, F., Bradley, R., Wang, H., and Shen, C., 2017, Synchronous precipitation reduction in the American Tropics associated with Heinrich 2: *Scientific Reports*, v. 7: 1126, p. 1–12, doi: 10.1038/s41598-017-11742-8.
- Mestas-Nuñez, A. M., Enfield, D. B., and Zhang, C., 2007, Water vapor fluxes over the Intra-Americas Sea: Seasonal and interannual variability and associations with rainfall: *Journal of Climate*, v. 20, no. 9, p. 1910-1922.
- Muñoz, E., Busalacchi, A. J., Nigam, S., and Ruiz-Barradas, A., 2008, Winter and summer structure of the Caribbean low-level jet: *Journal of Climate*, v. 21, no. 6, p. 1260-1276.
- Oster, J.L.; Warken, S.F.; Sekhon, N.; Arienzo, M.M.; Lachniet, M., 2019, Speleothem Paleoclimatology for the Caribbean, Central America, and North America. *Quaternary* 2019, 2, 5.

- Peterson, L.C., and Haug, G.H., 2006, Variability in the mean latitude of the Atlantic Intertropical Convergence Zone as recorded by riverine input of sediments to the Cariaco Basin (Venezuela): *Palaeogeography Palaeoclimatology Palaeoecology*, v. 234, p. 97–113.
- Philander, S.G.H., Gu, D., Lambert, G., Li, T., Halpern, D., Lau, N.C., Pacanowski, R.C., 1996, Why the ITCZ is mostly north of the equator. *Journal of climate*, 9(12), pp.2958– 2972.
- Poveda, G., Waylen, P.R., Pulwarty, R.S., 2006, Annual and inter-annual variability of the present climate in northern South America and southern Mesoamerica. *Palaeogeogr. Palaeoclimatol. Palaeoecol.* 234, 3–27.
- Shen, C.-C., Edwards, R.L., Cheng, H., Dorale, J.A., Thomas, R.B., Moran, S.B., Weinstein, S.E., and Edmonds, H.N., 2002, Uranium and thorium isotopic and concentration measurements by magnetic sector inductively coupled plasma mass spectrometry: *Chem. Geol.*, v. 185, p. 165–178.
- Shen, C.-C., Cheng, H., Edwards, R.L., Moran, S.B., Edmonds, H.N., Hoff, J.A., and Thomas, R.B., 2003, Measurement of attogram quantities of ^{231}Pa in dissolved and particulate fractions of seawater by isotope dilution thermal ionization mass spectroscopy: *Analytical Chemistry* , v. 75, p. 1075–1079.
- Shen, C.C., Wu, C.C., Cheng, H., Lawrence Edwards, R., Hsieh, Y. Te, Gallet, S., Chang, C.C., Li, T.Y., Lam, D.D., Kano, A., Hori, M., and Spötl, C., 2012, High-precision and high-resolution carbonate ^{230}Th dating by MC-ICP-MS with SEM protocols: *Geochimica et Cosmochimica Acta*, v. 99, p. 71–86, doi: 10.1016/j.gca.2012.09.018.
- Sutton, R.T., Hodson, D.L.R., 2005, Atlantic Ocean forcing of North American and European summer climate. *Science* 309, 115–118.
- Tremaine, D.M., Froelich, P.N. and Wang, Y., 2011, Speleothem calcite farmed in situ: Modern calibration of $\delta^{18}\text{O}$ and $\delta^{13}\text{C}$ paleoclimate proxies in a continuously-monitored natural cave system. *Geochimica et Cosmochimica Acta*, 75(17), pp.4929-4950.
- Vuille, M., Bradley, R.S., Healy, R., Werner, M., Hardy, D.R., Thompson, L.G., and Keimig, F., 2003, Modeling $\delta^{18}\text{O}$ in precipitation over the tropical Americas: 2. Simulation of the stable isotope signal in Andean ice cores: *Journal of Geophysical Research*, v. 108, p. 4175, doi: 10.1029/2001JD002039.
- Webster, J.W., Brook, G.A., Railsback, L.B., Cheng, H., Edwards, R.L., Alexander, C. and Reeder, P.P., 2007, Stalagmite evidence from Belize indicating significant droughts at the time of Preclassic Abandonment, the Maya Hiatus, and the Classic Maya collapse. *Palaeogeography, Palaeoclimatology, Palaeoecology*, 250(1-4), pp.1-17.

Winter, A., Miller, T., Kushnir, Y., Sinha, A., Timmermann, A., Jury, M.R., Gallup, C., Cheng, H.R.L., Edwards, R.L., 2011, Evidence for 800 years of North Atlantic multi-decadal variability from a Puerto Rican speleothem. *Earth Planet. Sci. Lett.* 308, 23–28.

6. Appendix

Table 1) CL Chronology

Sample	Distance cm	238U (ng/g) ^a	232Th (pg/g) ^a	d234U (per mil) ^b	[230Th/238U] activity	230Th/232Th ppm atomic	Age (yr ago) (uncorrected) ^c	Age (yr ago) (corrected) ^d	$\delta^{234}\text{U}$ initial (per mil) ^e	Age (yr BP) ^f (corrected) ^d
C-2	2	213	±4	219	±4	25.6	±1.2	540	±10	443
C-7	7	260	±5	92	±3	21.4	±1.8	814	±67	736
C-11.5	11.5	286	±6	329	±7	19	±3	1407	±61	1306
C-14	14	267	±5	285	±6	11	±2	1616	±62	1517
C2016-D	15.5	265	±5	193	±4	17.5	±1.7	2140	±30	2050
C. 2016-22	22	275	±5	869	±18	19.9	±1.9	2874	±20	2710
C-23	23	272	±5	857	±17	16.0	±2	3390	±20	3233

Notes:

^aReported errors for ²³⁸U and ²³²Th concentrations are estimated to be ±1% due to uncertainties in spike concentration; analytical uncertainties are smaller.

^b $\delta^{234}\text{U} = \left(\frac{^{234}\text{U}}{^{238}\text{U}} / \frac{^{234}\text{U}}{^{238}\text{U}}_{\text{standard}} - 1 \right) \times 1000$.

^c Ages are corrected for detrital ²³⁰Th assuming an initial ²³⁰Th/²³²Th of $(4.4 \pm 2.2) \times 10^{-6}$.

^d Ages are corrected for detrital ²³⁰Th assuming an initial ²³⁰Th/²³²Th of $(4.4 \pm 2.2) \times 10^{-6}$.

^e $\delta^{234}\text{U}_{\text{initial}}$ corrected was calculated based on $\frac{^{234}\text{U}}{^{238}\text{U}}$ age (T), i.e., $\delta^{234}\text{U}_{\text{initial}} = \delta^{234}\text{U}_{\text{measured}} \times e^{(\lambda^{234}\text{U} - \lambda^{238}\text{U})T}$, and T is corrected age.

^f B.P. stands for "Before Present" where the "Present" is defined as the January 1, 1950 C.E.

Decay constants for ²³⁰Th and ²³⁴U are from Cheng et al. (2013); decay constant for ²³⁸U is $1.55125 \times 10^{-10} \text{ yr}^{-1}$ (Jaffey et al., 1971).

Table 2) Fractionation Factor Calculations

	Isotope Fractionation Equation	$\delta_{18}O_w$ of regional precipitation (‰, VSMOW)	Cave Temperature (°C)	Calculated calcite $\delta_{18}O_c$ (‰, VPDB)
Afeck and Zaarur et al. (2014)	$1000 \ln \alpha_{calcite-water}$ = $15.63 * 10^3 / T$ - 23.29	-0.5 to -4.0	23.5 ± 0.5	~-1.3 – ~ -4.8
Hansen et al. (2019)	$1000 \ln \alpha_{calcite-water}$ = $16.52 * 10^3 / T$ - 26.14			~-1.2 – ~-4.6
Tremaine et al. (2011)	$1000 \ln \alpha_{calcite-water}$ = $16.1 * 10^3 / T$ - 24.6			~-2.8 – ~-6.3
Kim and O’Neil (1997)	$1000 \ln \alpha_{calcite-water}$ = $18.03 * 10^3 / T$ - 32.17			~-2.1 – ~-5.6

Table 2. Calcite $\delta_{18}O_c$ values were calculated using different isotope fractionation equations using measured regional precipitation $\delta_{18}O_w$ as assumed cave drip water $\delta_{18}O_w$ and cave temperatures. The annual regional precipitation $\delta_{18}O_w$ measurements range from precipitation low = -0.5‰ (VSMOW) to precipitation high = -4.0 ‰ (VSMOW) recorded from IAEA GNIP instrumental database from Cuba (2004-2015). Cave temperatures were estimated at ~1° C cooler than average temperature recorded to the nearest weather station in Matanzas, Cuba.

Table 3) Ages, $\delta^{18}\text{O}$, and $\delta^{13}\text{C}$ associated with stalagmite depth.

Depth from top (mm)	Age (yr BP: CE 2016)	$\delta^{18}\text{O}$	$\delta^{13}\text{C}$
0.5	322	-1.64	-1.97
1	328	-2.71	-2.12
1.5	333	-1.91	-2.21
2	338	-1.44	-3.32
2.5	343	-1.28	-5.01
3	349	-1.62	-5.26
3.5	354	-2.04	-5.53
4	359	-1.80	-5.51
4.5	365	-1.83	-5.72
5	370	-1.86	-6.86
5.5	375	-2.44	-7.28
6	380	-2.17	-6.39
6.5	386	-1.86	-6.62
7	391	-1.97	-7.36
7.5	396	-2.04	-7.52
8	402	-2.06	-8.09
8.5	407	-1.85	-8.08
9	412	-1.88	-8.14
9.5	417	-1.98	-7.96
10	423	-2.37	-7.45
10.5	428	-2.08	-7.61
11	433	-2.45	-8.28
11.5	439	-2.07	-8.42
12	444	-1.80	-8.37
12.5	449	-1.91	-8.54
13	454	-1.99	-8.27
13.5	460	-1.74	-8.12
14	465	-1.10	-8.09
14.5	470	-1.32	-8.17
15	476	-1.48	-8.21
15.5	481	-2.19	-8.74
16	486	-2.32	-8.49
16.5	492	-2.01	-8.45

17	497	-2.15	-8.70
17.5	502	-1.60	-8.02
18	507	-1.62	-8.00
18.5	513	-1.88	-8.33
19	518	-1.81	-7.81
19.5	523	-1.56	-7.83
20	529	-1.62	-7.56
20.5	532	-1.72	-7.79
21	535	-2.02	-7.51
21.5	538	-1.91	-7.93
22	541	-2.00	-8.11
22.5	544	-2.21	-7.79
23	547	-2.06	-7.69
23.5	550	-2.32	-7.63
24	554	-2.92	-8.14
24.5	557	-2.22	-7.81
25	560	-2.03	-7.85
25.5	563	-2.21	-8.02
26	566	-2.37	-8.23
26.5	569	-2.03	-8.15
27	572	-1.75	-8.33
27.5	575	-1.95	-8.23
28	578	-2.24	-8.33
28.5	581	-1.70	-8.09
29	585	-2.30	-8.41
29.5	588	-2.35	-8.36
30	591	-2.30	-8.12
30.5	594	-2.14	-8.29
31	597	-1.87	-7.99
31.5	600	-1.65	-7.66
32	603	-2.01	-7.88
32.5	606	-1.90	-7.92
33	609	-2.15	-7.69
33.5	611	-2.36	-8.18
34	614	-2.49	-8.30
34.5	617	-2.21	-8.20
35	620	-2.28	-8.09
35.5	623	-2.13	-8.10

36	626	-2.14	-7.90
36.5	629	-2.53	-8.12
37	632	-2.70	-8.02
37.5	635	-2.91	-7.81
38	638	-2.84	-7.75
38.5	641	-2.58	-7.38
39	644	-2.71	-7.65
39.5	647	-2.45	-7.51
40	650	-2.21	-7.69
40.5	653	-2.23	-7.58
41	656	-2.18	-7.78
41.5	659	-2.38	-7.63
42	662	-2.06	-7.53
42.5	665	-2.49	-7.70
43	668	-2.43	-7.95
43.5	671	-2.03	-7.87
44	674	-1.91	-7.95
44.5	677	-1.80	-7.34
45	680	-1.63	-7.51
45.5	683	-1.99	-7.79
46	686	-1.65	-7.56
46.5	689	-2.15	-7.81
47	692	-2.22	-7.87
47.5	695	-1.80	-7.99
48	698	-2.19	-8.10
48.5	701	-2.08	-7.88
49	704	-2.23	-8.08
49.5	707	-1.98	-7.95
50	710	-1.95	-8.22
50.5	713	-2.23	-8.47
51	716	-1.91	-8.47
51.5	719	-1.77	-8.41
52	722	-1.59	-8.29
52.5	725	-1.77	-8.06
53	728	-1.88	-8.25
53.5	731	-2.16	-8.30
54	734	-2.10	-8.56
54.5	737	-2.34	-8.76

55	740	-2.21	-8.55
55.5	743	-2.45	-8.34
56	746	-2.27	-8.29
56.5	749	-3.00	-8.24
57	752	-3.01	-8.09
57.5	755	-2.78	-8.24
58	758	-2.44	-8.33
58.5	761	-2.78	-8.25
59	764	-2.45	-8.15
59.5	767	-2.22	-7.95
60	770	-2.47	-8.16
60.5	773	-2.80	-8.27
61	776	-2.55	-8.20
61.5	779	-2.54	-8.39
62	782	-2.65	-8.40
62.5	786	-1.97	-8.39
63	789	-2.03	-8.55
63.5	792	-1.87	-8.36
64	795	-2.42	-8.86
64.5	798	-2.13	-8.56
65	801	-2.51	-8.49
65.5	804	-2.48	-8.68
66	807	-2.65	-8.80
66.5	810	-3.13	-8.49
67	814	-2.85	-8.44
67.5	817	-2.74	-8.54
68	820	-2.53	-8.59
68.5	823	-2.19	-8.83
69	826	-2.45	-8.81
69.5	829	-2.39	-8.70
70	832	-2.89	-8.87
70.5	837	-3.05	-8.89
71	842	-2.82	-8.64
71.5	847	-2.65	-8.60
72	852	-2.40	-8.41
72.5	857	-2.73	-8.57
73	862	-2.73	-8.26
73.5	867	-2.73	-8.32

74	872	-3.00	-8.27
74.5	877	-2.17	-8.08
75	882	-2.07	-8.21
75.5	886	-2.07	-8.24
76	891	-2.49	-8.38
76.5	896	-2.21	-8.30
77	901	-2.41	-7.99
77.5	906	-2.02	-7.96
78	911	-2.14	-8.09
78.5	916	-1.75	-8.09
79	921	-2.39	-8.24
79.5	926	-2.05	-8.37
80	931	-2.53	-8.62
80.5	936	-2.39	-8.43
81	941	-2.65	-8.42
81.5	946	-2.72	-8.67
82	952	-2.27	-8.34
82.5	957	-2.60	-8.66
83	962	-2.75	-8.66
83.5	967	-3.05	-8.80
84	972	-2.81	-8.70
84.5	978	-2.85	-8.64
85	983	-3.34	-8.62
85.5	988	-2.54	-8.50
86	993	-2.49	-8.51
86.5	999	-2.55	-8.38
87	1004	-2.23	-8.25
87.5	1009	-2.34	-8.25
88	1014	-2.15	-8.08
88.5	1019	-2.63	-8.17
89	1025	-3.02	-8.32
89.5	1030	-2.44	-8.34
90	1035	-2.30	-8.30
90.5	1040	-2.62	-8.41
91	1045	-2.90	-8.24
91.5	1050	-2.75	-8.11
92	1055	-2.66	-8.12
92.5	1060	-2.40	-8.04

93	1066	-2.60	-8.20
93.5	1071	-2.57	-8.19
94	1076	-2.51	-7.87
94.5	1081	-2.37	-8.05
95	1086	-3.03	-8.17
95.5	1091	-2.74	-8.14
96	1096	-2.60	-8.04
96.5	1101	-2.80	-8.21
97	1106	-2.91	-7.89
97.5	1111	-3.17	-8.15
98	1116	-3.48	-8.18
98.5	1121	-3.04	-7.85
99	1127	-2.74	-7.97
99.5	1132	-2.87	-8.15
100	1137	-2.60	-8.28
100.5	1142	-2.53	-8.58
101	1147	-2.45	-8.47
101.5	1152	-2.25	-8.19
102	1157	-2.53	-8.65
102.5	1162	-2.72	-8.72
103	1167	-2.73	-8.53
103.5	1172	-2.55	-8.28
104	1178	-2.60	-8.27
104.5	1183	-3.00	-8.20
105	1188	-3.23	-8.27
105.5	1193	-3.19	-8.36
106	1198	-2.84	-8.14
106.5	1203	-3.33	-7.99
107	1208	-3.07	-8.00
107.5	1213	-3.11	-8.05
108	1218	-3.24	-8.48
108.5	1223	-3.32	-8.57
109	1229	-2.99	-8.55
109.5	1234	-3.05	-8.27
110	1239	-3.60	-8.71
110.5	1245	-3.22	-8.72
111	1250	-2.83	-8.22
111.5	1256	-3.15	-8.52

112	1262	-2.97	-8.35
112.5	1268	-2.90	-8.37
113	1274	-2.88	-8.50
113.5	1280	-2.93	-8.36
114	1286	-2.46	-8.61
114.5	1291	-2.60	-8.55
115	1297	-2.76	-7.96
115.5	1303	-3.01	-8.07
116	1309	-3.06	-8.46
116.5	1315	-2.86	-8.45
117	1321	-2.33	-8.30
117.5	1326	-2.16	-8.21
118	1332	-2.42	-8.43
118.5	1338	-2.66	-8.24
119	1344	-2.95	-8.36
119.5	1350	-2.97	-8.30
120	1356	-2.84	-8.41
120.5	1362	-2.84	-8.35
121	1368	-2.77	-8.57
121.5	1374	-2.20	-8.43
122	1380	-2.45	-8.54
122.5	1385	-2.41	-8.60
123	1391	-2.24	-8.62
123.5	1397	-2.55	-8.63
124	1403	-2.94	-8.57
124.5	1409	-2.64	-8.68
125	1415	-2.85	-8.70
125.5	1421	-2.54	-8.36
126	1427	-2.42	-8.68
126.5	1433	-2.49	-8.34
127	1439	-2.26	-8.28
127.5	1445	-2.13	-8.28
128	1451	-2.26	-8.34
128.5	1457	-2.45	-8.12
129	1463	-2.66	-7.57
129.5	1469	-2.69	-8.02
130	1475	-2.72	-7.72
130.5	1481	-2.54	-7.79

131	1488	-2.42	-7.84
131.5	1494	-2.15	-8.15
132	1501	-1.54	-7.90
132.5	1508	-1.97	-8.17
133	1514	-2.28	-7.99
133.5	1521	-2.33	-8.04
134	1528	-2.40	-8.18
134.5	1534	-2.35	-7.95
135	1541	-1.79	-7.64
135.5	1547	-2.00	-7.81
136	1554	-1.96	-7.95
136.5	1561	-2.09	-8.14
137	1567	-2.48	-8.00
137.5	1574	-2.78	-8.34
138	1580	-2.49	-8.28
138.5	1587	-3.19	-8.25
139	1594	-2.96	-8.20
139.5	1600	-2.66	-8.14
140	1607	-2.41	-7.98
140.5	1623	-2.68	-7.52
141	1640	-2.35	-7.97
141.5	1657	-2.21	-7.81
142	1673	-2.33	-7.69
142.5	1690	-1.65	-7.21
143	1707	-1.44	-7.15
143.5	1723	-1.74	-7.55
144	1740	-1.84	-7.28
144.5	1757	-2.14	-7.58
145	1773	-2.44	-7.54
145.5	1790	-1.97	-7.40
146	1806	-2.14	-7.69
146.5	1823	-1.82	-7.82
147	1840	-2.21	-7.75
147.5	1856	-2.52	-7.66
148	1873	-2.51	-7.75
148.5	1890	-2.47	-7.91
149	1906	-2.80	-7.97
149.5	1923	-2.91	-8.09

150	1939	-2.96	-8.45
150.5	1951	-2.52	-8.13
151	1963	-2.27	-8.21
151.5	1975	-2.53	-8.18
152	1987	-2.37	-8.30
152.5	1999	-2.54	-8.59
153	2011	-1.96	-8.54
153.5	2023	-2.05	-8.68
154	2035	-1.93	-8.75
154.5	2047	-2.08	-8.86
155	2058	-2.55	-8.85
155.5	2070	-2.49	-9.02
156	2082	-1.91	-8.75
156.5	2094	-1.74	-8.83
157	2106	-2.14	-9.04
157.5	2118	-2.27	-8.91
158	2130	-2.30	-8.51
158.5	2142	-1.77	-8.69
159	2154	-1.82	-8.64
159.5	2166	-2.45	-8.53
160	2177	-2.79	-8.43
160.5	2184	-2.68	-8.41
161	2191	-2.76	-8.39
161.5	2198	-2.40	-7.94
162	2205	-2.51	-8.06
162.5	2211	-2.66	-8.60
163	2218	-2.52	-8.56
163.5	2225	-2.21	-8.76
164	2232	-2.36	-8.48
164.5	2239	-2.43	-8.83
165	2246	-2.53	-8.89
165.5	2252	-2.62	-8.69
166	2259	-2.91	-8.55
166.5	2266	-2.94	-8.18
167	2273	-2.56	-8.36
167.5	2280	-2.83	-8.15
168	2286	-2.52	-8.04
168.5	2293	-2.34	-8.02

169	2300	-2.59	-8.36
169.5	2307	-2.97	-8.64
170	2314	-3.21	-6.13
170.5	2320	-2.82	-8.47
171	2327	-2.88	-8.24
171.5	2333	-2.70	-8.46
172	2340	-2.80	-8.75
172.5	2346	-2.59	-8.81
173	2353	-2.67	-8.96
173.5	2359	-2.81	-9.14
174	2366	-2.72	-9.09
174.5	2372		
175	2379	-2.69	-9.60
175.5	2385	-2.66	-9.38
176	2392	-2.91	-9.00
176.5	2398	-3.10	-9.09
177	2405	-2.45	-9.13
177.5	2411	-2.68	-9.41
178	2418	-2.76	-9.38
178.5	2424	-2.73	-9.13
179	2431	-2.53	-8.80
179.5	2437	-2.52	-8.89
180	2444	-2.58	-8.60
180.5	2450	-2.68	-8.48
181	2456	-3.18	-8.57
181.5	2463	-3.10	-8.65
182	2469	-3.18	-9.02
182.5	2476	-3.36	-9.02
183	2482	-3.01	-8.93
183.5	2489	-2.83	-8.91
184	2495	-2.22	-8.66
184.5	2502	-2.42	-8.70
185	2508	-2.36	-8.94
185.5	2514	-2.22	-8.26
186	2521	-2.70	-8.80
186.5	2527	-2.73	-8.68
187	2534	-2.57	-8.58
187.5	2540	-2.53	-8.72

188	2547	-2.66	-8.11
188.5	2553	-2.10	-8.08
189	2560	-1.91	-8.17
189.5	2566	-1.91	-8.29
190	2573	-2.25	-8.36
190.5	2579	-2.25	-8.43
191	2585	-2.74	-8.06
191.5	2592	-3.05	-8.02
192	2598	-2.35	-8.15
192.5	2604	-2.75	-7.89
193	2611	-2.64	-7.47
193.5	2617	-2.36	-7.73
194	2624	-2.48	-8.07
194.5	2630	-2.67	-8.09
195	2636	-2.80	-7.86
195.5	2643	-2.54	-8.13
196	2649	-2.78	-8.27
196.5	2655	-2.69	-7.98
197	2662	-2.82	-8.17
197.5	2668	-2.96	-8.21
198	2675	-2.41	-8.07
198.5	2681	-2.64	-8.03
199	2687	-2.46	-8.33
199.5	2694	-2.12	-8.14
200	2700	-2.27	-8.43
200.5	2707	-2.34	-8.45
201	2713	-2.24	-8.52
201.5	2720	-2.86	-8.49
202	2726	-2.44	-8.39
202.5	2733	-2.42	-8.21
203	2739	-2.48	-8.22
203.5	2746	-2.54	-8.07
204	2752	-3.20	-7.85
204.5	2759	-3.52	-8.67
205	2766	-3.70	-8.57
205.5	2772	-2.27	-7.82
206	2779	-2.27	-7.63
206.5	2785	-2.60	-7.77

207	2792	-2.86	-8.21
207.5	2798	-2.54	-8.34
208	2805	-2.09	-8.16
208.5	2811	-1.69	-8.08
209	2818	-1.99	-8.41
209.5	2824	-2.27	-8.18
210	2831	-2.44	-7.69
210.5	2838	-1.68	-7.24
211	2846	-1.80	-7.09
211.5	2854	-2.44	-7.14
212	2861	-2.27	-7.42
212.5	2869	-2.49	-7.03
213	2876	-1.70	-6.64
213.5	2884	-1.89	-6.86
214	2891	-2.61	-7.10
214.5	2899	-2.35	-7.43
215	2906	-2.51	-7.25
215.5	2914	-2.73	-7.48
216	2922	-2.72	-7.50
216.5	2929	-2.47	-7.41
217	2937	-3.07	-7.98
217.5	2944	-2.56	-7.51
218	2952	-2.46	-7.50
218.5	2959	-2.90	-7.49
219	2967	-2.10	-7.63
219.5	2974	-2.24	-7.64
220	2982	-3.04	-7.71
220.5	3000	-2.50	-7.39
221	3018	-2.17	-7.51
221.5	3036	-2.91	-7.61
222	3053	-2.76	-7.86
222.5	3071	-2.21	-7.54
223	3089	-2.47	-7.58
223.5	3107	-2.74	-7.70
224	3125	-2.24	-7.59
224.5	3143	-2.26	-7.61
225	3161	-2.62	-7.66
225.5	3179	-2.34	-7.71

226	3197	-2.57	-7.67
226.5	3214	-2.74	-7.67
227	3232	-2.10	-7.44
227.5	3250	-2.37	-7.61
228	3268	-2.30	-8.08
228.5	3286	-1.67	-8.07
229	3304	-2.08	-7.63
229.5	3322	-1.92	-7.52
230	3340	-2.73	-7.39
230.5	3345	-2.47	-6.90
231	3350	-2.01	-7.00
231.5	3355	-2.15	-7.20
232	3361	-2.37	-7.24
232.5	3366	-2.36	-7.17
233	3371	-2.23	-7.46
233.5	3376	-2.19	-7.36
234	3382		
234.5	3387	-2.24	-7.33
235	3392	-2.43	-7.51
235.5	3397	-2.29	-7.37
236	3403	-2.53	-7.40
236.5	3408	-1.91	-6.25
237	3413	-1.86	-6.46
237.5	3418	-2.00	-6.55
238	3424	-1.94	-6.78
238.5	3429	-1.94	-6.99
239	3434	-1.77	-6.77
239.5	3439	-2.23	-7.22
240	3445	-2.47	-7.18
240.5	3450	-2.51	-7.12
241	3455	-2.59	-7.05
241.5	3460	-2.13	-7.06
242	3465	-2.20	-6.92
242.5	3470	-2.39	-7.08
243	3475	-2.21	-7.54
243.5	3480	-2.81	-8.77
244	3485	-3.38	-9.06
244.5	3490	-3.28	-9.52

245	3495	-3.35	-9.51
245.5	3500	-3.38	-9.48
246	3505	-3.46	-9.17
246.5	3510	-3.04	-9.07
247	3515	-3.54	-9.68
247.5	3520	-3.67	-9.09
248	3525	-3.53	-8.92
248.5	3530	-3.85	-8.89
249	3536	-3.52	-8.64
249.5	3541	-3.26	-8.45
250	3546	-2.81	-7.67
250.5	3551	-2.94	-7.67
251	3556	-2.56	-7.19
251.5	3561	-2.58	-7.12
252	3566	-2.28	-7.00
252.5	3571	-2.24	-7.09
253	3576	-2.07	-7.31
253.5	3581	-2.31	-7.34
254	3586	-2.21	-7.38
254.5	3591	-2.16	-7.17
255	3596	-2.38	-6.93
255.5	3601	-2.30	-7.02
256	3606	-2.31	-7.07
256.5	3612	-2.47	-6.82
257	3617	-2.38	-6.85
257.5	3622	-2.27	-7.07
258	3627	-2.37	-7.78
258.5	3632	-2.12	-7.24
259	3637	-1.97	-7.05
259.5	3642	-2.21	-7.30
260	3647	-1.80	-7.34
260.5	3652	-1.84	-6.91
261	3657	-2.08	-7.05
261.5	3662	-2.10	-7.18
262	3667	-2.10	-6.77
262.5	3672	-2.24	-6.94
263	3677	-2.93	-7.35
263.5	3682	-2.41	-7.04

264	3687	-2.10	-6.66
264.5	3692	-1.93	-7.03
265	3697	-2.08	-6.82
265.5	3701	-1.99	-6.87
266	3706	-1.95	-6.87
266.5	3711	-2.21	-6.72
267	3716	-1.92	-6.73
267.5	3721	-1.67	-6.62
268	3726	-2.20	-6.33
268.5	3731	-2.38	-6.82
269	3736	-1.79	-6.77
269.5	3741	-1.72	-6.78
270	3746	-2.02	-6.53